A PUSHOVER-BASED METHODOLOGY FOR THE SEISMIC VULNERABILITY ASSESSMENT OF LOW-TO MIDRISE REINFORCED CONCRETE STRUCTURES

A THESIS SUBMITTED TO
THE GRADUATE SCHOOL OF NATURAL AND APPLIED SCIENCES
OF
MIDDLE EAST TECHNICAL UNIVERSITY

BY

MEHMET FIRAT AYDIN

IN PARTIAL FULFILLMENT OF THE REQUIREMENTS
FOR
THE DEGREE OF MASTER OF SCIENCE
IN
CIVIL ENGINEERING

DECEMBER 2023

Approval of the thesis:

A PUSHOVER-BASED METHODOLOGY FOR THE SEISMIC VULNERABILITY ASSESSMENT OF LOW-TO MIDRISE REINFORCED CONCRETE STRUCTURES

submitted by **MEHMET FIRAT AYDIN** in partial fulfillment of the requirements for the degree of **Master of Science** i**n Civil Engineering, Middle East Technical University** by,

Prof. Dr. Halil Kalıpçılar
Dean, Graduate School of **Natural and Applied Sciences** _____

Prof. Dr. Erdem Canbay
Head of the Department, **Civil Engineering** _____

Prof. Dr. Murat Altuğ Erberik
Supervisor, **Civil Engineering, METU** _____

Examining Committee Members:

Prof. Dr. Ayşegül Askan Gundoğan
Civil Engineering, METU _____

Prof. Dr. Murat Altuğ Erberik
Civil Engineering, METU _____

Assoc. Prof. Dr. Mustafa Kerem Kockar
Civil Engineering, Hacettepe University _____

Assoc. Prof. Dr. Meltem Şenol Balaban
City and Regional Planning, METU _____

Assoc. Prof. Dr. Mustafa Tolga Yılmaz
Department Of Engineering Sciences, METU _____

Date: 11.12.2023

I hereby declare that all information in this document has been obtained and presented in accordance with academic rules and ethical conduct. I also declare that, as required by these rules and conduct, I have fully cited and referenced all material and results that are not original to this work.

Name Lastname : Mehmet Fırat Aydın

Signature :

ABSTRACT

A PUSHOVER-BASED METHODOLOGY FOR THE SEISMIC VULNERABILITY ASSESSMENT OF LOW-TO MIDRISE REINFORCED CONCRETE STRUCTURES

Aydın, Mehmet Fırat
Master of Science, Civil Engineering
Supervisor : Prof. Dr. Murat Altuğ Erberik

December 2023, 108 pages

The vulnerability assessment of structures under earthquake excitation is one of the key factors in determining the seismic resilience of a region. Generally, the response of equivalent single degree of freedom systems representing the characteristics of the interested building stock is analyzed by performing nonlinear time history analysis to minimize the computational effort. However, this analytical approach requires a considerable number of assumptions and simplifications to reflect the parameters that affect the behavior of the structure of the model which creates epistemic uncertainty.

In this study, an alternative methodology is proposed for rapid vulnerability assessment of low to midrise reinforced concrete structures. Firstly, representative 3D structural models are created concerning the number of stories, year of construction, and occupancy class (residential or non-residential) as well as structural deficiencies like the presence of heavy overhang, soft story, short column, plan, and vertical irregularity. In total, 4768 subclasses have been defined for low to midrise reinforced concrete structures with different characteristics and deficiencies. Secondly, static pushover analysis is conducted to obtain the idealized capacity

curves which represent fundamental nonlinearity parameters of the structural system such as ductility demand, post-yield stiffness ratio, etc. together with dynamic modal properties of the system. Then, statistical approaches are implemented by using the outputs of the generated database to predict the parameters of idealized capacity curves of every low to midrise reinforced concrete structure rather than creating structure-specific models and performing static nonlinear procedures. In this manner, one can easily perform the capacity spectrum method by using generated capacity curves or perform an idealized single degree of freedom nonlinear time history analysis by using hysteretic relationships with predicted nonlinearity parameters.

The generated algorithm can be implemented for a much larger domain of low to midrise reinforced concrete structures including the defects that cause most of the observed damage after severe earthquakes. This study attempts to decrease the computation time significantly together with increasing the modeling accuracy for the regional seismic vulnerability assessment procedures.

Keywords: Reinforced Concrete Structures, Structural Dynamics, Pushover Analysis, Idealization of Capacity Curves, Risk Assessment

ÖZ

AZ-ORTA KATLI BETONARME YAPILARIN SİSMİK HASARGÖREBİLİRLİK DEĞERLENDİRMESİ İÇİN STATIK İTME ANALIZINE DAYALI BİR YÖNTEM

Aydın, Mehmet Fırat
Yüksek Lisans, İnşaat Mühendisliği
Tez Yöneticisi: Prof. Dr. Murat Altuğ Erberik

Aralık 2023, 108 sayfa

Yapıların deprem etkisi altındaki hasar görebilirlik değerlendirmesi, bir bölgenin sismik dirençliliğini belirlemede kilit faktörlerden biridir. Genel olarak, hesaplama süresini en aza indirmek için gözönünde bulundurulan bina stoğunun karakteristik özelliklerini temsil eden eşdeger tek serbestlik dereceli sistemlerin tepkisi, zaman tanım alanında doğrusal olmayan analiz yapılarak belirlenir. Ancak bu analitik yaklaşım, idealize edilmiş modele yapının davranışını yansıtmak için epistemik belirsizlikler yaratan bir çok varsayımda bulunur.

Bu çalışmada, az ve orta katlı betonarme yapıların hasargörebilirlik değerlendirmesi için daha hızlı bir alternatif metodoloji önerilmektedir. İlk olarak kat sayısı, yapım yılı, kullanım sınıfı (konut veya konut dışı), ağır çıkma, yumuşak kat, kısa kolon, plan ve düşey duzensizlik gibi yapısal noksanlıklara ilişkin temsili üç boyutlu yapısal modeller oluşturulmuştur. Farklı özellik ve düzensizliklere sahip az ve orta katlı betonarme yapılar için toplamda 4768 alt sınıf tanımlanmıştır. Sonrasında, sistemin dinamik modal ozellikleri ile birlikte süneklik talebi, akma sonrası rijitlik oranı vb. gibi doğrusal olmayan parametrelerini temsil eden idealize edilmiş kapasite eğrilerini elde etmek için statik itme analizi yapılmıştır. Daha sonrasında, belirli bir yapı sınıfına özgü modeller oluşturmak ve doğrusal olmayan prosedürler

gerçekleştirmek yerine, az ve orta katlı her çeşit betonarme yapının idealleştirilmiş kapasite eğrilerinin parametrelerini tahmin etmek için oluşturulan veritabanının çıktılarını kullanarak istatistiksel yaklaşımlar uygulanmıştır. Bu sayede, üretilen kapasite eğrilerini kullanarak kapasite spektrumu yöntemi kolayca uygulanabilir veya tahmin edilen doğrusal olmayan parametrelerle histeretik ilişkileri kullanarak idealize edilmiş tek serbestlik dereceli zaman tanım alanında doğrusal olmayan analiz gerçekleştirilebilir.

Oluşturulan algoritma, şiddetli depremlerden sonra gözlemlenen hasarın çoğunluğuna sebebiyet veren kusurlar da dahil olmak üzere, tek kattan 12 katlı betonarme yapılara kadar çok daha geniş bir küme için uygulanabilir. Bu çalışma, sismik hasar görebilirlik değerlendirme prosedürleri için modelleme etkinliğini artırmakla birlikte hesaplama süresini de önemli ölçüde azaltmaktadır.

Anahtar Kelimeler: Betonarme Yapılar, Yapı Dinamiği, Statik İtme Analizi, Kapasite Eğrilerinin İdealizasyonu, Risk Tayini

Dedicated to all the loved ones who lost their lives in the 1999 Kocaeli Earthquake...

1999 Kocaeli depreminde hayatını kaybetmiş tüm depremzedelere adanmıştır…

ACKNOWLEDGMENTS

I wish to express my profound gratitude to my esteemed thesis advisor, Prof. Dr. Murat Altuğ Erberik, for his invaluable guidance and unwavering support throughout the entirety of my academic pursuit. His expertise, encouragement, and commitment to my scholarly development have been pivotal in shaping the trajectory of my research and overall academic endeavors. I am truly appreciative of his dedication to fostering an environment of intellectual growth and their meticulous guidance in navigating the complexities of my research. His mentorship has not only enriched my academic experience but has also significantly contributed to the refinement of my analytical and research skills.

I would also like to express my sincere gratitude to Prof. Dr. Ayşegül Askan for her abiding support in all situations, for entrusting me with various responsibilities, and for affording me the chance to mold my academic trajectory through the creation of novel opportunities.

I would like to thank to respected members of the thesis jury, Assoc. Prof. Mustafa Kerem Koçkar, Assoc. Prof. Meltem Şenol Balaban, and Assoc. Prof. Mustafa Tolga Yılmaz for their valuable contributions and kind wishes. I also appreciate their insightful observations and attention to pertinent details.

I express my gratitude to my esteemed colleague, Abdullah Altındal, for his invaluable support in introducing me to the realm of earthquake engineering during my undergraduate years. His encouragement to delve into research in this field and academic guidance has been instrumental in shaping my journey up to the present. I eagerly anticipate celebrating the numerous accomplishments you will undoubtedly attain in your future endeavors and look forward to engaging in numerous collaborative ventures with you

The technical assistance of my friends Mr. Said Batuhan Bilmez and Mr. Berkay Akçören is gratefully acknowledged. Your support has been indispensable in facilitating the swift completion of the entire coding and analysis process; I am

deeply grateful for your assistance, without which accomplishing this task with such efficiency would not have been possible.

I wish to extend my heartfelt appreciation to my esteemed friends Umut Aydemir, Mehmet Serkan Aydın, and Çağkan Doğan, who consistently provided unwavering support in both my academic and social endeavors. They attentively listened to my concerns and demonstrated enthusiasm exceeding my own when it came to contemplating my future.

Finally, my deepest gratitude to my family, whose eternal support and unconditional love have been the bedrock of my personal and academic journey. Their encouragement and sacrifices have been instrumental in shaping my character and providing me with the resilience to overcome challenges. I am profoundly appreciative of the sacrifices made on my behalf and the steadfast belief in my capabilities. Their enduring support has been a source of inspiration, fostering an environment conducive to my growth and achievements. In acknowledging the integral role my family has played, I am truly thankful for their selfless commitment to my well-being and success.

This work is partially funded by the National Earthquake Research Program of AFAD, Turkiye under grant number UDAP-C-21-59.

TABLE OF CONTENTS

LIST OF TABLES

TABLES

LIST OF FIGURES

FIGURES

LIST OF ABBREVIATIONS

1D One dimensional

2D Two dimensional

3D Three dimensional

API Application programming interface

BH Beam height

BW Beam width

CDR Central damage ratio

CSM Capacity spectrum method

CW Column width

DPM Damage probability matrix

DR Damage ratio

DS Damage state

E Modulus of Elasticity

EAFZ East Anatolian Fault Zone

GIS Geographic Information System

LHS Latin hypercube sampling

LS Limit state

MDR Mean damage ratio

MMI Modified Mercalli Intensity scale

MN Mean

MPA Modal pushover analysis

NAFZ North Anatolian Fault Zone

NLTHA Non-linear time history analysis

PE Probability of exceedance

PGA Peak ground acceleration

PGV Peak ground velocity

RC reinforced concrete

RSA Response spectrum analysis

SDOF Single degree of freedom

SRSS Square Root of the Sum of the Squares

ST Story

STD Standard deviation

LIST OF SYMBOLS

$\mu = Ductility\ ratio$

$\eta = Strength\ reduction\ factor$

$k = Stifness$

$K_e = Elastic\ stiffness$

$E = Modulus\ of\ elasticity$

$f_{ck} = Characteristic\ strength\ of\ concrete$

$v = Poisson\ ratio$

$\alpha_t = Thermal\ expansion\ coefficient$

$\alpha_s = Post\ yield\ stiffness\ ratio$

$\alpha_c = Post\ capping\ stiffness\ ratio$

$\epsilon_0 = Strain\ of\ concrete\ model\ at\ the\ ultimate\ force\ capacity$

$\epsilon_{ult} = Strain\ of\ concrete\ model\ at\ the\ crushing\ stage$

$\gamma_{concrete} = Unit\ weight\ of\ concrete$

$\delta_y = Yield\ displacement$

$\delta_c = Capping\ displacement$

$\delta_r = Displacement\ where\ residual\ capacity\ starts$

$t_{slab} = Slab\ thickness$

$n_{max} = Maximum\ number\ of\ reinforcement\ in\ a\ surface$

$n_{min} = Minimum\ number\ of\ reinforcement\ in\ a\ surface$

$cw = Column\ width$

$l_{span,x} = Span\ length\ in\ X - direction$

$l_{span,y} = Span\ length\ in\ Y - direction$

$CR_{org} = Original\ location\ of\ the\ center\ of\ rigidity$

$CR_{new} = New\ location\ of\ the\ center\ of\ rigidity$

$ecc = Eccentricity$

CHAPTER 1

INTRODUCTION

With hundreds of kilometers of active faults located in densely populated cities with vulnerable building stocks, Turkiye is a country that is prone to earthquakes. The past earthquakes in Erzincan, Kocaeli, Van, Elazig, and Seferihisar (Samos) allowed us to witness the effects of this fact—which we should never forget. The North Anatolian Fault Zone (NAFZ) has caused numerous severe earthquakes over the past century, but the East Anatolian Fault Zone (EAFZ), the second major fault system, has been relatively quiet for a long time. Two incidents in the northeast parts, the Mw6.0 Karakocan Elazig earthquake in 2010 and the Mw6.8 Sivrice Elazig earthquake in 2020 shattered this period of silence. Three years later, on February 6, 2023, two catastrophic earthquakes with epicenters near Kahramanmaras city in Turkiye struck the southwestern portions of the EAFZ within 9 hours. The first event, with a Mw7.7 epicenter near the Pazarcik sub-province of Kahramanmaras, happened at 04:17 local time (01:17 GMT). Approximately 400 kilometers of the fault line ruptured during this earthquake, which had a devastating impact on 11 populated cities nearby and caused severe property damage and fatalities. The author of this thesis report is one of many researchers who have been in the earthquake region since the first week of the tragedy in an endeavor to collect perishable field data. According to post-earthquake reconnaissance assessments, this significant earthquake sequence caused diverse amounts of damage to hundreds of thousands of buildings with various construction typologies. These earthquakes also made it abundantly evident that structures in high-risk areas of the nation should be identified as soon as possible, and that work on retrofitting or urban transformation projects should begin right once.

There are two approaches to doing this examination. A comprehensive assessment is one of these. The building project is sourced from municipalities or other pertinent entities for this assessment. Following a thorough inspection, the building's deficiencies for the original project are identified. Then, information regarding the quality of the building's construction materials is gathered by using a variety of processes, such as taking samples from structural elements. The building is then precisely modeled in a computer system, and the region's seismic risk is assessed by allocating a risk score. The building's seismic resistance is assessed as part of this scoring system. However, depending on how quickly the application is processed, this process for one single building could take days, weeks, or even months to finish. But as earthquakes have demonstrated, it is impossible to do a thorough analysis of Turkiye's whole building stock due to their ability to concurrently affect hundreds of thousands of buildings across dozens of regions.

It is advisable to perform the thorough analysis outlined in the preceding paragraph, beginning with the major characteristics of the building stock. Rapid assessment is another evaluation method that can be used to accomplish this preliminary assessment. Instead of modeling the structure in detail and conducting in-depth studies, these methods allow for the appraisal of the building based on a few basic characteristics that can be ascertained by inspecting them from the outside. Although creating representative models to simulate the response of the building under consideration causes a considerable loss of accuracy, it significantly reduces the computational time. The extensive area impacted by the recent Kahramanmaraş earthquake sequence has made it abundantly evident that an urgent assessment of our nation's building stock is required. The building stock can then be renovated more swiftly by taking actions like structural strengthening or urban transformation.

1.1 Literature Survey

Numerous researchers have been interested in seismic loss estimation for several decades. Freeman (1932) made the first attempts to construct seismic loss estimation studies for insurance firms. However, after the early 1970s, there was a sharp rise in interest in seismic loss estimation studies. Since then, an extensive variety of approaches for estimating seismic loss have been presented.

In general, seismic loss assessment methodologies have three vital components: seismic hazard quantification, building fragility, and socioeconomic vulnerability. Firstly, there are two ways to predict ground motion demand: deterministic (Küçükçoban, 2004, Bal et al., 2008, Demircioglu et al., 2010, Ugurhan et al., 2011) and probabilistic seismic hazard assessments (Smyth, 2004, Crowley and Bommer, 2006). Building fragility, the second component of loss estimation can be derived through extensive structural examination of a particular building (Aslani and Miranda, 2005). Damage probability matrices or fragility curves created for a building stock can also be used for a set of structures in broader areas (Akkar et al., 2005, Ay and Erberik, 2008, Erberik, 2008a, Erberik, 2008b, Askan and Yücemen, 2010). Finally, empirical (Wald et al., 2008), analytical (FEMA, 2003), or hybrid (Wald et al., 2008, Wyss et al., 2009) methodologies can be used to construct casualty and economic loss estimating equations. This thesis specifically focuses on structural fragility.

As stated in the introduction of this section, it is not possible to analyze each building in Turkiye's building stock in detail to determine its vulnerability to earthquakes due to the enormous number to deal with. In such situations, it is crucial to use easier and more practical techniques without losing the required accuracy.

Performance-based earthquake engineering studies include a variety of analysis techniques, ranging from linear static analysis to nonlinear time history analysis applications through a step-by-step increase in information level, analysis complexity, and analysis time. The success rate offered by linear elastic analysis

techniques is extremely poor, especially as they are unable to give a genuine assessment of the structure's plastic behavior. For this reason, it is necessary to use nonlinear analysis techniques, namely nonlinear static pushover analysis and nonlinear time history analysis. These approaches, however, can be extremely time-consuming since they need an excessive number of parameters to both represent the behavior of the building under earthquake excitation and attempt to solve a problem involving sophisticated nonlinear interactions.

The use of representative equivalent single degree of freedom systems (ESDOF) in dynamic and static structural analysis for damage estimation is a common and long-used method. Gulkan and Sozen (1974) and Shibata and Sozen (1978) suggested a substitute structure technique, which was an implementation of the ESDOF concept, in the 1970s. When working with a large number of structures, employing representative ESDOF systems of structures is desirable for maximum efficiency. This simplified approach has long been employed in earthquake engineering applications; it dates back to Biggs (1964), and many studies have since followed (e.g., Saiidi and Sozen, 1981; Fajfar and Fischinger, 1988; Qi and Moehle, 1991; Aschheim and Black, 2000). Akkar et al. (2005) obtained 32 represented buildings of Turkish Reinforced Concrete frames with 2- to 5-stories. Building response was described as SDOF system response. Kircil and Polat (2006) created fragility curves for Istanbul's mid-rise RC Frame buildings. Buildings of three, five, and seven stories were designed following the 1975 version of the Turkish seismic code. Building reaction was modeled in 2D, and fragility curves were generated. Korkmaz and Johnson (2007) investigated the probabilistic approach for defining seismic structural behavior in the represented 7-story RC concrete frame buildings. Using FEMA 440 (American Society of Civil Engineers, 2005), the building was idealized as an SDOF system. Erberik (2008a) evaluated typical RC Frame Low-rise and Mid-rise structures in Turkey using the Düzce damage database following the Düzce (1999) Earthquake. The building's response was idealized as an SDOF system. Ozmen et al. (2010) studied the vulnerability of 2, 4, and 7-storey RC Frame buildings built according to pre-2000 seismic codes using fragility curves. The

structure is modeled as SDOF and they generated 96 equivalent models following ATC-40 and FEMA 440.

Nonlinear static pushover analysis, another popular approach to determining structural vulnerability, can offer accurate approximations of where inelastic behavior is located. Estimates of the maximum deformation cannot be obtained from pushover analysis alone. For this reason, additional research has to be done. It's critical to understand that pushover studies do not aim to forecast how a structure will react to an earthquake. Also, nonlinear dynamic analysis is unlikely to be able to forecast the outcome. Any analytical technique, including pushover, must at the very least be suitable for design. Because of its ease of use, inelastic static analysis, often known as pushover analysis, has been the recommended technique for evaluating seismic performance. Nonlinear material properties are immediately incorporated into the static analysis. The Displacement Coefficient Method (FEMA356, 2000), and the Capacity Spectrum Method (ATC40, 1996) are examples of inelastic static analysis techniques.

On the other hand, buildings are modeled in a computer system to create a one-, two-, or three-dimensional numerical simulation as part of the highest-level analysis technique known as nonlinear time history analysis. Next, each computer model is examined individually in the time history under several strong ground motion records that might be indicative of seismic activity at the building's site. A set of representative ground motion recordings that take uncertainties and variations in intensity, frequency, and duration characteristics into consideration must also be available. Computational times in this procedure may rise dramatically, particularly as the number of strong ground motions used and the complexity of the model both increase. Because of this, when the building stock is large, such in-depth analyses are rarely preferred in regional risk estimations. In these situations, idealized one-dimensional single degree of freedom systems are established for the buildings under consideration instead of a detailed modeling of the buildings. In this approach, even though the prediction's accuracy declines dramatically, the computation time is greatly decreased, and the task is intended to be finished rapidly. However, to

perform these idealized analyses, the basic parameters that will represent the inelastic behavior of the considered structure class must be obtained through pushover analysis results.

In pushover analysis, an approximation of an analysis technique, the structure is subjected to a height-wise distribution of progressively increasing lateral forces until a desired displacement is achieved. Pushover analysis approximates a force-displacement curve of the overall structure by superimposing a sequence of consecutive elastic analyses. First, gravity loads are applied to a two- or three-dimensional model that comprises bilinear or trilinear load-deformation diagrams of all lateral force-resisting parts. Next, a predetermined pattern of lateral loads is applied, dispersed throughout the height of the building. Up until certain members yield, the lateral forces are increased. Lateral forces are raised once more until more members yield, and the structural model is adjusted to reflect the decreased stiffness of yielding members. The procedure is carried out repeatedly until the building's top control displacement reaches a predetermined degree of deformation or the structure becomes unstable. The global capacity curve is obtained by plotting the roof displacement against base shear.

Pushover analysis can be done in displacement- or force-controlled ways. Force-controlled pushover procedures apply the entire load combination as required; hence, when the load is known, force-controlled procedures should be employed (e.g., gravity loading). Additionally, because of the development of mechanisms and P-delta effects, target displacement may be linked with a very modest positive or even negative lateral stiffness in force-controlled pushover procedures, which can lead to numerical issues that compromise the correctness of the results. To get around these issues, pushover analysis is typically carried out as displacement-controlled. Specific drifts are sought in displacement-controlled procedures (similar to seismic loading) when the imposed load's magnitude is unknown in advance. Until the control displacement reaches a certain value, the load combination's intensity is adjusted as needed. Typically, the displacement of the roof at the mass center of the structure is selected as the control displacement. For a performance check, the estimations of

inelastic strength and deformation demands derived from the internal forces and deformations estimated at the target displacement must be compared to the available capacity.

Due to its conceptual simplicity and ease of computation, pushover analysis has been the method of choice for major rehabilitation recommendations and regulations when evaluating the seismic performance of structures. Pushover analysis makes it possible to follow the progression of the structure's overall capacity curve as well as the sequence of yielding and failure at the member and structural levels. Despite pushover analysis's advantages over elastic analysis techniques, it is important to recognize the limitations of existing pushover procedures as well as their underlying assumptions and the precision of pushover forecasts. The accuracy of pushover results is affected by several significant factors, including the estimation of the target displacement, the choice of lateral load patterns, and the detection of failure mechanisms resulting from higher modes of vibration.

Adaptive processes were used to overcome the shortcomings of nonlinear static procedures. Paret et al. (1996) advocated performing various pushover analyses with force distributions proportional to the mass matrix multiplication and elastic mode forms corresponding to different modes. They developed the Modal Criticality Index (MCI) to determine the vibration mode most likely to cause structural failure. Sasaki et al. (1998) extended the MCI and suggested the Multi-Mode Pushover (MMP) Procedure to account for the effects of higher modes. Many additional researchers investigated adaptive pushover processes, taking into account higher mode effects and varied lateral load patterns (for example, Gupta and Kunnath 2000, Aydınoğlu 2003, Antoniou and Pinho 2004a and 2004b).

Antoniou and Pinho (2004a) conducted a study to determine the advantages and limitations of force-based pushover procedures that are both adaptive and non-adaptive. The study concludes that, although force-based adaptive pushover appears to have a better conceptual foundation, it has a slight advantage over its non-adaptive

counterpart. This is especially true when it comes to estimating building deformation patterns, which are not well predicted by either model.

The pushover analysis method that has been developed by Chopra and Goel (2002) preserves the conceptual simplicity and computational appeal of the existing processes with invariant force distribution. It is based on structural dynamics theory. The seismic demand resulting from individual terms in the modal expansion of the effective earthquake forces is compared in this modal pushover analysis (MPA) with a thorough non-linear response history analysis. It is shown that MPA estimates building responses well into the inelastic range with a degree of accuracy comparable to that of response spectrum analysis (RSA) in estimating the peak response of elastic systems. As a result, the MPA process has sufficient accuracy for use in the evaluation and design of buildings. Chopra et al. (2004) introduced a modified form of MPA known as MMPA, in which the inelastic response obtained from first-mode pushover analysis is merged with the elastic contribution of higher modes. Because the influence of higher modes is assumed to be linear elastic in MMPA, pushover analysis for higher modes of vibration is not required. As a result, the inelastic response of the fundamental mode is merged with the elastic contribution of higher modes, as determined by individual linear response history analysis.

The review of Seifi et al. (2008) on the state of pushover analysis development allows for the following findings to be made. To begin with, pushover analysis offers a solution to complex capacity and deformation estimation issues for specific structural types. Second, most research has been done on two-dimensional R/C frame structures. Therefore, further research on these topics is needed as the application of pushover for high-rise frames, steel structures, and 3D constructions is not well studied.

According to Leslie (2013), The approach seems sound and comprehensive as a result, but there are still many issues that need to be worked out, such as how to incorporate the torsional impacts of structures. The approach essentially considers only the fundamental mode, presuming it to be the major reaction, and does not take

into consideration the effects of higher modes. This is the most addressed (but still unsolved) issue. For buildings with periods longer than one second, the differences resulting from higher mode effects begin to be felt. Even though numerous research publications have suggested different approaches to adding higher modes (rather than just combining the lateral effects corresponding to each mode), a standard approach has not yet been established and integrated into software packages.

1.2 Scope and Motivation

Turkiye is home to a variety of architectural styles, from non-engineered brick village homes to high-rise reinforced concrete (RC) frame structures. However, the test bed for this investigation has been determined to be RC frame buildings. According to post-earthquake reconnaissance assessments, this choice was made primarily because it was found to be the building type that was most susceptible to seismic damage. Additionally, it is the most common building form in risky city centers. For this purpose, rapid risk assessment of RC buildings is of great importance.

Technically speaking, it is not feasible to thoroughly study each building in the building stock while researching to ascertain the regional earthquake risk. In these circumstances, it is vital to employ easier and more practical methods. The primary goal of this thesis study is to raise the accuracy rate in rapid estimating processes without lengthening the evaluation period. To idealize the behavior of RC buildings, a new study has been carried out in this context. In this context, only the detached structures were taken into consideration. The general characteristics of Turkiye's building stock and construction practices were gathered from statistical studies for this project, and numerous computer models that could represent these qualities were developed. The nonlinear behavior of RC buildings under the influence of earthquakes was then idealized by examining the outputs produced by these models. The parameter set presented as the outputs of this study can be used as a basis for rapid risk identification studies in Turkiye.

1.3 Outline of the Thesis Study

This thesis study is focused on a methodology based on static pushover analysis for seismic vulnerability assessment of low to mid-rise reinforced concrete structures. It includes 5 chapters in total.

Chapter 1 is the introduction, which highlights the gap in the literature that the thesis topic of choice targets, provides an overview of the vulnerability studies that have been done, and suggests further steps to focus on the current study.

An explanation of all the fundamental steps in this thesis is provided in Chapter 2. Initially, the factors that directly influence how a building responds to an earthquake excitation are identified. Following that, a compilation of statistical studies was made to describe the distribution and prevalence of these criteria in Turkiye's building stock. After that, a sensitivity analysis was conducted concerning the model input parameters, and the specifics of the computer models that had been constructed were explained.

Chapter 3 provides a full explanation of the steps involved in creating idealized capacity curves that will depict the inelastic behavior of the structures under consideration. This context includes the steps involved in the analysis, the idealization of the acquired curves by the application of techniques found in the literature, and the parts that provide examples of practical applications for the results.

In Chapter 4, the author provides an overview of the procedures followed in an urban seismic resilience determination project in the Türkoğlu district of Kahramanmaraş during the author's thesis work. The efficacy of the new database created for this study is compared with values commonly found in the literature.

Finally, Chapter 5 is the conclusion section that discusses the results obtained from this study, its contributions to the literature, and the parts that need to be improved in further studies.

CHAPTER 2

GENERATION OF BUILDING MODELS

The most important phase in this study is to develop models that accurately reflect the architectural characteristics of Turkish building stock. It should be stated that a reliable seismic risk assessment can only be established by implementing the region-specific construction features to the structural models. The most likely and frequent types of irregularities to be found in structures should be reflected in the models for this purpose, together with the commonly favored building techniques and material properties in the Turkish construction sector. Initially, the most effective parameters in the seismic behavior of buildings should be determined.

2.1 Structural Parameters Affecting Seismic Response

2.1.1 Number of Stories

The elongation of the building's natural vibration period is since adding floors results in a considerably higher increase in the mass of the structure than in its lateral stiffness. Accordingly, the capacity of the structure requires additional requirements to meet this demand as the displacement demands of the building steadily increase under the same ground motion intensity. As a result, the seismic vulnerability of buildings increases in tandem with the number of stories they have.

2.1.2 Construction Year

One of the most important determinants of the regulations to which the building was designed is the date it was constructed. With advancements in both material properties and contemporary design approaches, new buildings can be designed and

constructed with a lot more seismic safety over time. This makes the building's construction year one of the most important factors affecting how the structure will respond to earthquakes. Işık (2021) showed that each regulation change has positive effects on the behavior of the buildings as a result of his comparison study, taking into account the minimum conditions imposed by the earthquake regulations in Turkiye.

2.1.3 Occupancy Class

The occupancy class of the building is one of the important parameters taken into consideration in TBEC (2018) regulations to determine the building importance factor and the earthquake design method to be followed. The major difference between the use of the building being either residential or non-residential is generally the increase in the dead and live loads carried by the building. For example, a government institution may have many more items or electronic devices than a standard residence. This increases the mass of the building without changing the lateral stiffness.

2.1.4 Presence of Shear Walls

Shear wall buildings, according to Badaux and Peter (2000), exhibit significant stiffness, lateral resistance, and little inter-story deformation. Fintel (1995) observed that shear walls were particularly effective at limiting structural and nonstructural damage to buildings during the Chile Earthquake, even though cracking was seen in them.

Shear walls greatly increase the lateral stiffness of the system without appreciably increasing the dead load. The system's period of vibration decreases as a result. While this causes an increase in the building's force demands when regarded from the perspective of spectral acceleration, it significantly lowers the demands when evaluated from the perspective of spectral displacement.

Although it causes the building to carry more load due to the stiffness it gains, it reduces the displacement demands considerably because the moment of inertia is much larger than the columns. In terms of lowering the displacement demands, the presence of shear walls has a very favorable and considerable impact on how the structure behaves.

Figure 1. Failure of a shear wall from Kahramanmaraş

2.1.5 Material Properties

The behavior of the building is greatly influenced by the yield capacity, ductility, modulus of elasticity, and many other material properties employed during its construction. In light of both the improvements in the production technologies of construction materials and the studies carried out in the literature to understand material behavior, the overall material uncertainty is gradually decreasing. For example, the differences between hand-mixed concrete and ready-mixed concrete, or between a brittle old reinforcement and a ductile reinforcement produced with high technology, should be effectively reflected in the model to simulate a more reliable behavior for idealized structural models.

2.1.6 Reinforcement Details

The amount, detailing, and quality of the reinforcement used in RC buildings are critical for the ultimate limit state of a structure. Although adequately reinforced and properly detailed RC elements behave much more ductile and exhibit enhanced performance, on the contrary, older structures with inadequate detailing show a much inferior and brittle behavior.

Figure 2. Deformed and plain reinforcement details from Antakya, Hatay

2.1.7 Structural Irregularities

2.1.7.1 Existence of Excessive Overhangs

An overhang is a form of vertical irregularity that is present in a considerable number of buildings in the Turkish building stock, and it is utilized to increase the floor area on the stories above the ground story. It can be regarded as a heavy overhang if the cantilever portion is 1 meter or longer (by inspection).

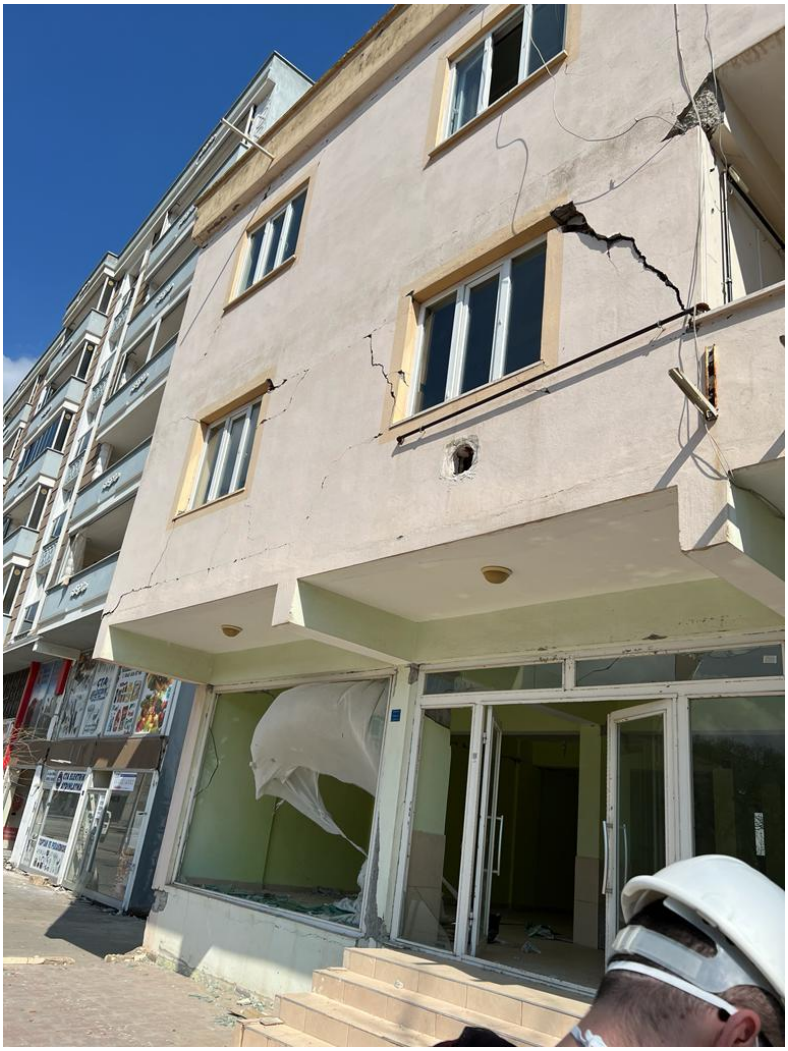

Figure 3. A real-life example of excessive overhangs from Turkoglu, Kahramanmaraş

2.1.7.2 Soft/Weak Story

A "soft story" is a form of vertical irregularity where there is a considerable lateral stiffness change between any two consecutive stories (especially if it takes place between the ground and the first stories). In the case of a significant lateral strength difference between any two consecutive stories, this vertical irregularity is defined as a “weak story”. It is simple to inspect the soft story irregularity in a building through the street survey. For buildings where the ground story is used for commercial purposes but the above stories are for residential purposes, the ground story can be considered a soft story. (Fig. 4). From outside the building, it is more challenging to identify the "weak story" Weak story irregularity can be inspected in cases when a structure has different structural features or material properties between floors (for instance, lower floor RC and upper floor masonry construction).

Figure 4. A real-life example of a building with a soft ground story

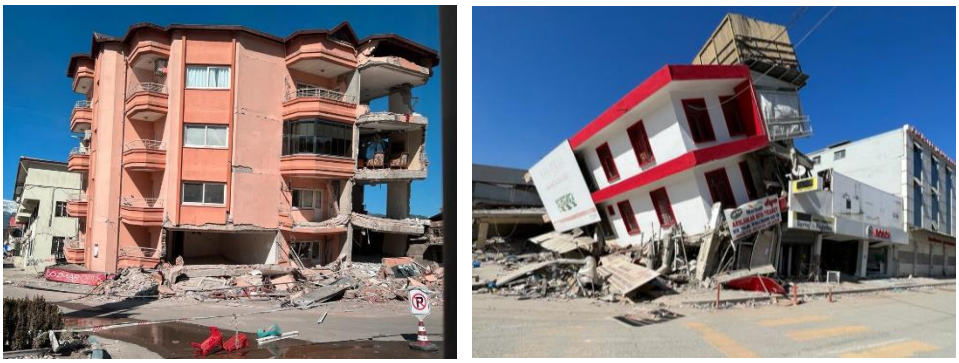

Figure 5. Failures due to the soft story on the ground floor from Antakya, Hatay

2.1.7.3 Short Column

A short column is easy to specify from outside of the structure. The "short column" class includes captive columns between window openings, especially in public and governmental buildings. This structural deficiency can be encountered on any floor of the structure but is typically found on the ground floor.

Figure 6. A real-life example of a building with short (captive) columns

2.1.7.4 Plan Irregularity

In terms of building geometry, plan irregularity in structures can only be checked from the outside. Plan regularity refers to a building's plan geometry, which might be rectangular or nearly rectangular with small projections. In addition, L, C, U, E, etc. On the other hand, plan irregularity refers to structures with more complex plan geometries containing large projections (for instance L, C, U, or E-shaped) and having axes that are not parallel to one another.

Figure 7. Examples of plan regularity and irregularity in floor plans

Figure 8. Severely damaged hotel building with plan irregularity from Adıyaman

2.1.7.5 Vertical Irregularity

Vertical irregularity includes all significant changes through the elevation (vertical axis) of the building. It is generally easy to identify from outside the building. This type of structural irregularity is particularly encountered in multiple-story RC buildings. Some examples of vertical irregularity are presented in Fig. 9.

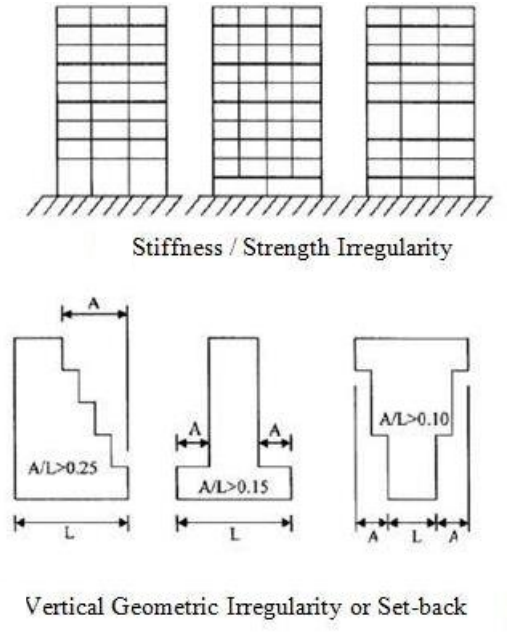

Figure 9. Types of Vertical Irregularities in Buildings (Titiksh, 2017)

2.2 Statistical Evaluation of Structural Parameters for Turkish Building Stock

Structural simulations should be performed employing a sampling strategy when creating idealized models for each RC frame typology. This study utilizes the Latin Hypercube sample (LHS) Method, a segmentation-based sample technique that works with many variables (Mc Kay et al. 1979). The LHS method has been widely used in structural earthquake engineering research over the past 20 years due to its

advantage over the Monte Carlo approach in terms of computational cost and its ability to produce estimated findings for the desired accuracy level with a constrained number of samplings (Erberik and Elnashai 2004, Erberik 2008a). Therefore, 20 samples are created for each random variable using the LHS sampling strategy in this study for each building subclass. According to Erberik (2008a), this sample size is sufficient for expressing structural variability in vulnerability analysis.

2.2.1 Constraints on the Sampling Process

To preserve the physical basis of the scenarios to be reflected in the numerical models and the realism of the samples obtained, some restrictions have to be defined in this process. This is the only way to represent the characteristic features of the building classes to which they belong. Firstly, limitations for some types of irregularities can be listed as follows.

- The existence of heavy cantilevers cannot occur in single-story structures. It can only be observed from 2 or more stories.
- Soft story irregularity cannot be observed in single-story structures. It can be observed from 2 or more stories.
- Vertical irregularity cannot occur in 1 and 2-story structures. It can be observed in structures with 3 or more stories.
- The presence of shear walls is generally not common in structures with 1-4 stories. Even if such a case exists, shear walls cannot be fully activated to create a hybrid system behavior. So, it has been decided that shear walls can be implemented in the structural models with 5 stories or above.

Next, the constraints on the geometrical properties of structures can be summarized as follows.

- Beam depth cannot be smaller than 0.40 m following the TBEC-2018 and 0.30 m following the previous seismic codes (ABYYHY-1975, ABYYHY-1998, TEC-2007).
- The beam width cannot be smaller than 0.20 m according to ABYYHY-1975 (1975) and 0.25 m according to the later versions of Turkish seismic codes (ABYYHY-1998), TEC-2007, TBEC-2018).
- Physically, the beam width cannot be greater than the beam depth to represent the regular RC frame behavior.
- The minimum column dimension is limited to 0.30 m following the TBEC-2018 and 0.25 m following the previous seismic codes (ABYYHY-1975, ABYYHY-1998, TEC-2007).
- Slab thickness cannot be smaller than 8 cm (Bal, 2007).

2.2.2 Sampling Procedure

First of all, following the purpose of this thesis study, it has been decided to work on buildings from 1 to 12 floors to take into account residential-type structures that are frequently encountered in earthquake zones in Turkiye. Then, building models are created by considering the design and construction to be between the years 1975-1998, 1998-2007, 2007-2018, and 2018, respectively, to cover the regulations of the last four Turkish seismic codes. Afterward, occupancy class (i.e. residential or non-residential use) is accepted as a variable to determine the purpose of building use. Finally, in terms of structural irregularities, soft story, short column, and vertical irregularities are considered Boolean, which is a form of data meant to represent the two truth values of logic and Boolean algebra. It can have one of two potential values, typically marked true or false.

In total, 14 parameters were sampled by assuming a statistical distribution that can represent the characteristics of the Turkish RC frame buildings within the scope of this thesis study. There exist many studies that aim to determine the inherent geometrical and material properties of existing structures in different provinces of Turkiye (Bal et al., 2007, Azak et al., 2014, Ozmen et al., 2015, Meral, 2018). The sampled parameters and respective distributions can be summarized as follows:

- Cantilever Ratio: The normal distribution suggested by Bal et al. (2007) is selected with a mean value of 0.091 and a standard deviation of 0.091 in terms of the ratio of the cantilever length to the considered floor length since this study provides a distribution independent from the number of stories of the structure.
- Plan Irregularity: Since a distribution for this type of irregularity in terms of eccentricity does not exist in the literature with sufficient sampling based on Turkish building data, a uniform distribution ranging between 1% and 20% was used.
- Shear Wall: To reflect the construction characteristics of Turkish building stock, it was decided to apply a uniform distribution between 0.5% and 2%.
- Concrete and Steel Grades: Normal distributions suggested by Ozmen et al. (2015) are selected since this study provides independent distributions concerning the number of stories and the construction years (Table 1).

Table 1. Statistical properties of construction materials suggested by Ozmen et al. (2015)

Number of Stories and Construction Year	Parameter	Mean (MPa)	St. Dev (MPa)
1-2ST <1998	f_{yk}	220	0
1-2ST <1998	f_{ck}	17.5	0.9
3-5ST <1998	f_{yk}	222.1	20.4
3-5ST <1998	f_{ck}	17.9	1.4
6-8ST <1998	f_{yk}	242.6	63.8
6-8ST <1998	f_{ck}	16.8	2.3
1-2ST >1998	f_{yk}	420	0
1-2ST >1998	f_{ck}	24	3.1
3-5ST >1998	f_{yk}	405.3	52.4
3-5ST >1998	f_{ck}	25.2	3.7
6-8ST >1998	f_{yk}	415.7	29.2
6-8ST >1998	f_{ck}	28.7	3.7

- Reinforcement Ratios: Normal distributions suggested by Ozmen et al. (2015) are selected since this study provides independent distributions concerning the number of stories and the construction years (Table 2).

Table 2. Statistical properties of reinforcement ratios of structural elements suggested by Ozmen et al. (2015)

Number of Stories and Construction Year	Parameter	Mean	St. Dev	Lower Bound
1-2ST <1998	ρ_{column}	0.0096	0.0012	0.0072
3-5ST <1998	ρ_{column}	0.0100	0.0019	0.0062
6-8ST <1998	ρ_{column}	0.0114	0.0033	0.0048
1-2ST >1998	ρ_{column}	0.0105	0.0012	0.0081
3-5ST >1998	ρ_{column}	0.0109	0.0019	0.0071
6-8ST >1998	ρ_{column}	0.0113	0.0021	0.0071
1-2ST <1998	ρ_{beam}	0.0051	0.0020	0.0031
3-5ST <1998	ρ_{beam}	0.0059	0.0028	0.0031
6-8ST <1998	ρ_{beam}	0.0068	0.0033	0.0035
1-2ST >1998	ρ_{beam}	0.0044	0.0010	0.0034
3-5ST >1998	ρ_{beam}	0.0051	0.0020	0.0031
6-8ST >1998	ρ_{beam}	0.0072	0.0033	0.0039

- Geometrical Properties of the Structure: Story height, building dimensions, and span lengths were sampled by using the statistical distributions suggested by Ay et al. (2014). The building length in the long direction is calculated by multiplying the sampled short length (L_{short}) with the sampled ratio of the short to the long length of the floor (L_{short}/L_{long}). Statistical parameters of the suggested normal distributions including the story height (H_{story}) and span lengths for both short ($L_{span,\ short}$) and long ($L_{span,\ long}$) directions can be summarized as seen in Table 3.

  Table 3. Statistical properties of geometrical characteristics of the structure suggested by Ay et al. (2014)

Parameter	Mean (m)	St. Dev (m)
L_{short}	9.58	3.64
L_{short}/L_{long}	0.73	0.18
$L_{span,\ long}$	3.59	0.61
$L_{span,\ short}$	3.51	0.74
H_{story}	2.71	0.20

- Geometrical Properties of Structural Elements: Normal distributions suggested by Ozmen et al. (2015) are selected since this study provides independent distributions concerning the number of stories and the construction years. Statistical parameters of the suggested normal distributions including the beam height (BH), beam width (BW), and the ratio of the total column area to the total floor area (A_{column} / A_{floor}) can be summarized as seen in Table 4.

Table 4. Statistical properties of geometrical characteristics of structural elements suggested by Ozmen et al. (2015)

Number of Stories and Construction Year	Variable	Mean	St. Dev
1-2ST <1998	BH (m)	0.5529	0.033
3-5ST <1998	BH (m)	0.5310	0.0857
6-8ST <1998	BH (m)	0.5301	0.1375
1-2ST >1998	BH (m)	0.4972	0.0377
3-5ST >1998	BH (m)	0.4568	0.1019
6-8ST >1998	BH (m)	0.5002	0.0739
1-2ST <1998	BW (m)	0.2188	0.0131
3-5ST <1998	BW (m)	0.2297	0.0752
6-8ST <1998	BW (m)	0.2694	0.1331
1-2ST >1998	BW (m)	0.2613	0.0523
3-5ST >1998	BW (m)	0.2958	0.0956
6-8ST >1998	BW (m)	0.2745	0.0601
1-2ST <1998	A_{column} / A_{floor}	0.0172	0.0065
3-5ST <1998	A_{column} / A_{floor}	0.0185	0.0048
6-8ST <1998	A_{column} / A_{floor}	0.0230	0.0065
1-2ST >1998	A_{column} / A_{floor}	0.0210	0.0067
3-5ST >1998	A_{column} / A_{floor}	0.0220	0.0057
6-8ST >1998	A_{column} / A_{floor}	0.0250	0.0081

A summary of all distributions used within the scope of statistical sampling is presented in Table 5. A total of 4768 building subclasses were identified after taking into account the building's structural irregularities, occupancy class, year of construction, and number of stories. A total of 95360 structural models were prepared within the SAP2000 analysis software by generating 20 samples for every building subclass. Then nonlinear static pushover analyses are applied to each numerical model.

Table 5. Summary of the properties of random variables in the sampling process

Input Parameter	Unit	Distribution Type	Lower Bound	Upper Bound	Used Reference
Number of Stories	-	Uniform	1	12	-
Construction Year	-	Uniform	1975	2023	-
Usage Type	-	Uniform	R	N	-
Cantilever Ratio	Percent(%)	Normal	5	-	Bal, 2007
Soft Story	Binary	Uniform	False	True	-
Short Column	Binary	Uniform	False	True	-
Plan Irregularity	Percent(%)	Uniform	1	20	-
Vertical Irregularity	Binary	Uniform	False	True	-
Shear Wall Ratio	Percent(%)	Uniform	0.5	2	-
Concrete Strength	MPa	Normal	2	-	Ozmen, 2015
Rebar Strength	MPa	Normal	150	-	Ozmen, 2015
Beam Reinforcement Ratio	Percent	Normal	0.3	-	Ozmen, 2015
Column Reinforcement Ratio	Percent	Normal	0.5	-	Ozmen, 2015
Short Length of Floor Plan	Meters	Normal	-	-	Ay, 2014
Plan Aspect Ratio(Short/Long)	Percent(%)	Normal	-	100	Ay, 2014
Span Length in Long Dir.	Meters	Normal	-	-	Ay, 2014
Span Length in Short Dir.	Meters	Normal			Ay, 2014
Story Height	Meters	Normal	-	-	Ay, 2014
Beam Height	Meters	Normal	0.30	-	Ozmen, 2015
Beam Width	Meters	Normal	0.20	-	Ozmen, 2015
Column Area Ratio	Percent	Normal	0		Ozmen, 2015
Slab Thickness	Meters	Normal	0.08	-	Meral, 2018

2.3 Modeling details

Within the scope of this thesis, the SAP2000 structural analysis platform (CSi, 1998) has been used because it is widely preferred in structural engineering applications, provides a comprehensive interface for developing three-dimensional models, and enables external intervention with computer code.

The CSi Application Programming Interface (API) is a potent tool that gives users the ability to automate many of the procedures necessary to create, examine, and design models as well as to get customized analysis and design outcomes. Additionally, it enables users to connect SAP2000 to other applications, opening a channel for the two-way exchange of model data with other software.

The API can be used to access SAP2000 in the most popular programming languages. The major programming languages C#, Python, MATLAB, and Visual Basic for Applications (VBA), which are used in applications like Microsoft Excel, all provide this capability. In this thesis, the API was used over the Python programming language.

2.3.1 Assigning the Structural Parameters to the Computer Model

2.3.1.1 Code Compliance

In Turkish Earthquake Code regulations, the minimum conditions required for the earthquake-resistant design and construction of buildings are presented by taking into account the seismic intensity level of the region of interest. There have been 8 revisions in total, including 1947, 1953, 1961, 1968, 1975, 1998, 2007, and 2018, which is the current version. The progress of the earthquake-resistant design in Turkiye is directly related to the advancements in structural analysis and construction technologies and experiences gained from post-earthquake field observations of destructive earthquakes in the past.

First, the code regulations governing the seismic design of the building concerning the construction year of the structure are selected. The latest four versions of the Turkish earthquake codes have been considered.

Table 6. Considered earthquake codes of Turkiye

Year	Name of the Code	Abbreviation (in Turkish)
1975	Specification for Structures to be Built in Disaster Areas	ABYYHY-1975
1998	Specification for Structures to be Built in Disaster Areas	ABYYHY-1998
2007	Turkish Earthquake Code	DBYBHY-2007
2018	Turkiye Building Earthquake Code	TBDY-2018

2.3.1.2 Concrete Grade

The Python code written by the author of this thesis selects the most suitable standard concrete grade by concerning the specified concrete strength as the preliminary step. For example, with a stated concrete strength of 27.7 MPa, the program selects C25-grade concrete. Then, the isotropic properties, which are the modulus of elasticity, Poisson ratio, and coefficient of thermal expansion, were modified concerning TS500 regulations as follows.

$$Modulus\ of\ Elasticity\ (E) = 3250\sqrt{f_{ck}} + 14000 \quad (2.1)$$

$$Poisson\ Ratio\ (\nu) = 0.2 \quad (2.2)$$

$$Thermal\ Expansion\ Coefficient\ (\alpha_t) = 1 \times 10^{-5}\ /°C \quad (2.3)$$

Next, the stress-strain relationship suggested by Mander (1998) is implemented with unconfined strain $\epsilon_0 \cong 0.002$ and $\epsilon_{ult} \cong 0.005$. Finally, Takeda's (1970) hysteretic model is implemented for the force-displacement behavior of the members.

2.3.1.3 Steel Rebar Strength

The standard TS500 states upper and lower limits for the ultimate strength to be 15% to 35% than the yield strength. So, the upper limit is selected since most used rebar types, especially the older ones with smaller strength values, generally yield to the upper boundary stated by the provisions.

While the parametric stress-strain curve with a generic shape for the strain hardening section (simple model), which is accessible in SAP2000, was implemented for longitudinal and transverse reinforcement, the Mander (1998) model, which is available in SAP2000, was used for both confined and unconfined concrete. For the parametric strain data, which comprise the strain at the beginning of strain hardening and final strain capacity, Caltrans default controlling strain values—which depend on bar size—were employed.

2.3.1.4 Stiffness Modifiers

Stiffness modifiers suggested in TBEC2018 are used for beams, columns, and shear walls. Those modification factors can be summarized as follows.

- Bending stiffness is accepted as 35% of the uncracked section for beams,
- Bending stiffness is accepted as 70% of the uncracked section for columns,
- Bending stiffness is accepted as 50%, and shear area is accepted as 50% of the uncracked section for shear walls modeled with wide column analogy.

2.3.1.5 Load Assignments

Dead load on floor slabs is simply calculated by multiplying the unit weight of concrete with the input slab thickness as follows.

$$D = \gamma_{concrete} \times t_{slab} = 25 * t_{slab}\ kN/m^2 \quad (2.4)$$

Live load on floor slabs is calculated by considering the occupancy class of the building model (i.e., residential buildings or non-residential buildings which generally includes schools, hospitals, and governmental buildings following the definitions of TS-498)

The standard TS-498 declares a live load value as $2\ kN/m^2$ for residential buildings, as $3.5\ kN/m^2$ for classrooms, hospital examination rooms, and as $5\ kN/m^2$ for corridors of schools and hospitals. Since it is not possible to identify which one to use in the vast number of building simulations, the value $5\ kN/m^2$ has been selected for non-residential buildings as a conservative value.

Live load participation factors have been stated in TBEC-2018 as 30% for residential buildings and 60% for non-residential buildings. The load assignments for live loads have been made following these recommendations.

2.3.1.6 Reinforcement Assignments

According to the standard TS-500, the clear cover must be at least 25 mm. Hence, this value has been employed in all the models in this study.

2.3.1.6.1 Beam Reinforcement

Beam reinforcement density represents the amount of tension reinforcement for beam sections. Tension reinforcement is provided directly by multiplying the cross-sectional area of the beam with the stated reinforcement ratio.

Compression reinforcement is the most effective parameter for ductile beam design. In this manner, structures designed after the TEC1998 code regulations were most likely to have more ductile beams. To quantify this difference.

- For structures having a construction year later than 2018, compression reinforcement is assumed to be placed with an equal amount of the provided tension reinforcement.

- For structures designed by using the codes ABYYHY-1998 and TEC-2007, the selected compression reinforcement ratio is assumed to be half of the reinforcement that is placed for the tension zone.
- For structures built earlier than the year 1998, compression reinforcement is provided only as $2\phi 12$ hangers.

2.3.1.6.2 Column Longitudinal Reinforcement

SAP2000 offers 12-, 14-, 16-, 20-, 26- and 28-mm diameter rebars for SI Units with an example abbreviation of "26d". Therefore, the maximum diameter is selected as 28 mm. The minimum diameter for column longitudinal reinforcement is stated as 12 mm in TS500.

Spacing between longitudinal bars is the required parameter to find the optimum placement of rebars concerning the column reinforcement ratio. According to the TS-500 regulations, by neglecting the maximum diameter of the aggregate used in the concrete mix parameter, the minimum spacing between two longitudinal bars cannot be smaller than 20 mm or the selected bar diameter. This condition is the governing factor of the maximum number of rebars in one face of the column.

The current earthquake code provides a limitation for lateral spacing between stirrups and hooks to be smaller than 25 times the stirrup diameter, which corresponds to at most 200 mm spacing for 8 mm diameter stirrups. So, there must be a longitudinal bar in every 200 mm within the section of the member. This condition is the governing factor of the minimum number of reinforcements in one face of the column for the latest codes. However, previous codes do not provide limitations for such cases.

In the following paragraphs, an example case study is presented by designing a 45x45 cm column with a reinforcement ratio of 1.5%, for a building constructed in 2010.

The maximum number of rebars that are provided in one face for 28 mm diameter bars can be calculated as follows. Maximum diameter rebar gives the most critical result since spacing cannot be smaller than the rebar diameter.

$$n_{max} = \left(\frac{(cw + 0.028 - 0.025 * 2)}{(0.028 + 0.028)}\right) = 7$$

In the above calculation, parameter *cw* is the column width. A minimum number of rebars that is provided on one face for 28 mm diameter bars can be calculated as follows. Since the building is assumed to be constructed by the 2007 code, lateral spacing requirement between shear reinforcement legs governs. In this case, minimum longitudinal bar diameter becomes more critical since it increases the spacing between bars.

$$n_{min} = \left(\frac{(cw + 0.2 - 0.025 * 2)}{(0.012 + 0.2)}\right) = 3$$

Therefore, the written code has upper and lower boundaries for reinforcement selection. There are $7\phi 28\ bars$ and $3\phi 12\ bars$. Then, the code calculates the obtained reinforcement ratio for all possible alternatives between the boundaries. Finally, the code selects the optimum reinforcement design that has the closest reinforcement ratio for the stated one; i.e. 1.5%.

Starting from $3\phi 12, 3\phi 14, 3\phi 16$ to $7\phi 20, 7\phi 26, 7\phi 28$, the optimum output is $4\phi 16\ bars$ with a reinforcement ratio of 1.589%.

2.3.1.6.3 Column Lateral (Shear) Reinforcement

For lateral reinforcement, $\phi 8$ diameter stirrups have been selected since it is generally the most preferred diameter. Ductile failure is obtained by ensuring flexural failure in columns. Therefore, the earthquake code in force concerning the construction year of the structure is selected as the governing parameter. On the one hand, it should be stated that newer codes ensure ductile failure by providing more

shear reinforcement. On the other hand, older structures generally have the minimum amount of shear reinforcement according to statistical surveys (Ozmen 2015, Meral 2018).

For TBEC-2018,

- the number of legs is set to be equal to the minimum requirement for lateral spacing between stirrups "a",
- 8d rebars are selected as lateral reinforcement,
- spacing is selected as 50 mm, which is the minimum value recommended in the TBEC-2018.

For TEC-2007,

- the number of legs is set to be equal to the minimum requirement for lateral spacing between stirrups "a",
- 8d rebars are selected as lateral reinforcement,
- spacing is selected as 100 mm, which is the mean of observed values in Ozmen (2015) and Meral (2018).

For ABYYHY-1998,

- the number of legs is set to be equal to two, which means no hooks are used.
- 8d rebars are selected as lateral reinforcement,
- and spacing is selected as 100 mm, which is the mean of observed values in Ozmen (2015) and Meral (2018).

For ABYYHY-1975,

- the number of legs is set to be equal to two, which means no hooks are used,
- 8d rebars are selected as lateral reinforcement,
- and spacing is selected as 200 mm, which is the mean of observed values in Ozmen (2015) and Meral (2018). This is also the minimum requirement of the code.

2.3.1.6.4 Shear Wall Longitudinal Reinforcement

The same procedure for column reinforcement design is repeated for the width of the shear wall. The reinforcement ratio of the wall is assumed to be equal to the column reinforcement ratio. Then, the obtained output is provided for the short face of the wall. The number of reinforcement bars is multiplied by the aspect ratio of the wall to determine the number of longitudinal reinforcements provided in the long face of the wall.

As an example case study, if a 45x270 cm shear wall with a reinforcement ratio of 1.5% is considered in a building constructed in the year 2010, the optimum output is obtained as $4\phi16\ bars$ for the short face of the wall as found in Section 2.3.1.6.2. Noting that the aspect ratio can be calculated as

$$Aspect\ ratio = \frac{270}{45} = 6$$

the long face of the shear wall has $24\phi16\ bars$.

2.3.1.6.5 Shear Wall Lateral (Shear) Reinforcement

The number of legs in the cross-section is selected to be equal to the number of bars in one face to provide adequate shear resistance to ensure ductile failure.

2.3.1.7 Rigid End Zones

Member end offsets are assigned to structural elements by using the connectivity with a rigid zone factor of 1.0.

2.3.1.8 Shear Walls

Shear wall area in one direction is usually provided between 0.5% and 2% of the total floor area in the Turkish construction practice (Bal, 2007). In addition, shear walls are generally assigned to the edges of the floor plan since plan irregularity is also an input for this pushover analysis hence the corner columns of the structure are deleted on all floors. Using core shear walls in the center of the floor plan can be misleading for the analysis results in the presence of plan irregularity as core walls will reduce the eccentricity occurring in the system by restricting the movement of the center of rigidity due to providing a rigid zone.

Shear wall width is selected as the same as the beam width for easier section assignments in the modeling process.

The program controls the number of shear walls in one direction to match the input wall area ratio. A function creates all alternatives by changing the number of walls together with changing the wall length starting from the lower limit of 6 times the wall width. This is the aspect ratio condition stated in TBEC-2018 to an upper limit of two times the span length in the considered direction.

Shear walls are modeled with equivalent frame elements to define nonlinear flexural hinges since the SAP2000 program does not offer area hinges yet. (Figure 10). Also, it is a fact that area sections increase the analysis time significantly.

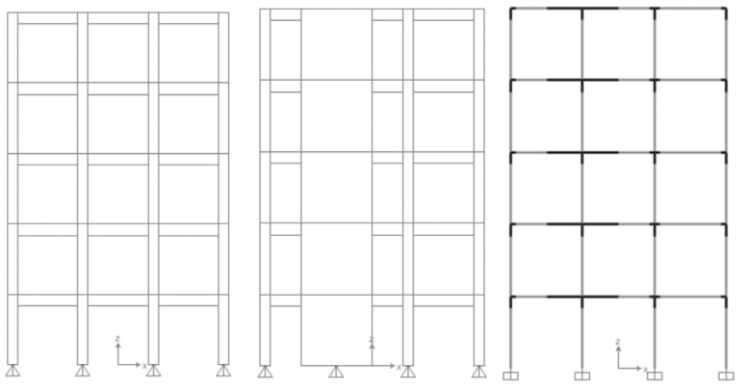

Figure 10. Graphical representation of the shear wall modeling

2.3.1.9 Hinges

Frame hinges have been automatically generated from built-in ASCE41-13 (2014) tables in SAP2000 rather than using an external section analyzer to reduce computation time for each model. If user-defined hinges are employed, hinge properties like damage states and scale factors of the backbone curve must be calculated manually. This case increases the computation time and raises a need for using another software to analyze the section.

For built-in hinges, SAP2000 automatically calculates the bending capacity and respective damage states by considering the reinforcement and cross-section properties of the corresponding section. It should be noted that the generated properties should be checked whether it is logical or not.

Limiting the negative stiffness ratio is accepted as 1, which means stiffness can be degraded completely. In addition, the option “hinges can drop load during unloading” is enabled during the analyses.

For beams, M3 hinges are employed since the axial load can be considered negligible. However, columns have P-M2-M3 hinges to consider the N-M interaction of the column sections.

To consider brittle shear failures especially can be seen in the presence of short column deficiency, nonductile shear hinges have been defined in column members in both directions.

2.3.1.10 Pushover Load Cases

First, a static nonlinear vertical pushover load pattern is defined to provide a starting point for the lateral pushover analysis. After that, hinges are formed by concerning the load-sharing patterns of each structural element in the vertical pushover load case.

Then a modal analysis is performed on the system to understand the dynamic behavior of the structure. After obtaining the mode shape results by focusing on the mass center of each floor and obtaining the mass participation ratios of each considered mode, two lateral load patterns are defined for the horizontal axes by simply multiplying the mode shape vectors for each direction with the respective mass participation ratios to represent the dominancy of the considered mode. Then, all modal force vectors are combined by using the SRSS technique. This procedure generally gives more accurate results for predicting the damage observed in the 'exact' analysis since it can represent the torsion effect due to possible irregularities in the structure.

The following options have been preferred for the solution control mechanism:

- Results are saved at multiple states with a minimum of 50 and a maximum of 200 steps with an adequate step size to represent the state of the structure under step loading.
- Default solution control parameters are preferred except disabling event-to-event stepping to observe a full failure path without convergence problems.
- Displacement-controlled pushover analysis is applied with a monitored maximum roof drift of 6%. This drift is tracked by using a generalized displacement definition including the displacements of each joint in the top story in the considered lateral direction.
- P-delta effects are taken into consideration.

2.3.2 Representation of Structural Irregularities

2.3.2.1 Heavy Cantilevers

First, the cantilever span length is calculated for both axes by using the cantilever ratio for each model. This ratio is defined as the percentage of the length of the cantilever part to the total length of the interested direction of the building. For instance, if a cantilever ratio is selected as 0.2, the span length of the cantilever elements in a structure having 3 spans with a span length of 3 meters in short direction and 4 spans with a span length of 5 meters can be calculated as follows:

$$l_{span,x} = x \times dx \times CR = 3 \times 3 \times 0.2 = 1.8\, meters$$
$$l_{span,y} = y \times dy \times CR = 4 \times 5 \times 0.2 = 4\, meters$$

Note that, the span length of cantilever elements is limited to the average span length in the interested direction to provide stability to the model.

Second, cantilever beams along the horizontal orthogonal axes are added concerning the span length. Then, beams interconnecting the added cantilever beams are defined. Lastly, columns connecting cantilever beams of different floor levels are added. Figure 11 presents the comparison of a building model having heavy cantilevers with a regular building model.

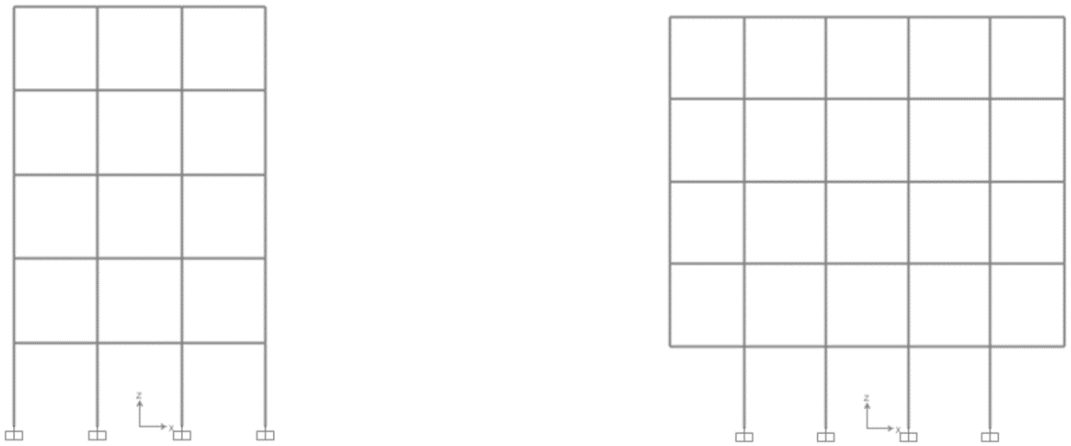

Figure 11. Comparison of a building having heavy cantilevers with a regular building

2.3.2.2 Soft Story

Literature generally suggests a ratio of soft to regular story height between 1.12 and 1.28 (Bal 2007, Ay 2014, Ozmen 2015, Meral 2018). However, due to the absence of infill walls on the ground floor, this ratio is increased to represent this effect by 50%. For example, a structure having a story height of 3 m, the height of the soft story on the ground floor becomes 4.5 m (see Figure 12).

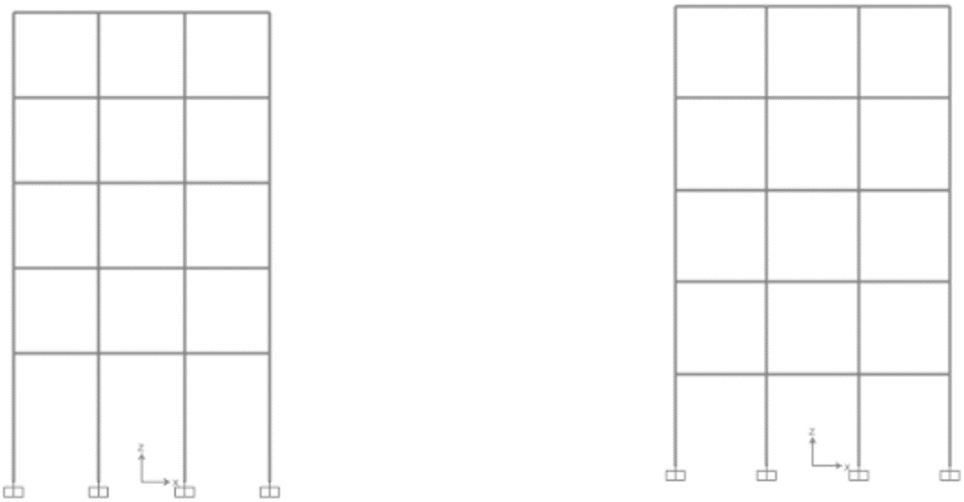

Figure 12. Comparison of a building having a soft story irregularity with a regular building

2.3.2.3 Plan Irregularity

Plan irregularity is implemented by considering the eccentricity ratio. First, all the columns are tabulated concerning their coordinates, heights, and respective stiffnesses for both horizontal axes. Numbering of the columns on an example floor plan is provided in Figure 13 and the corresponding summary of column positions and stiffness contributions is listed in Table 7.

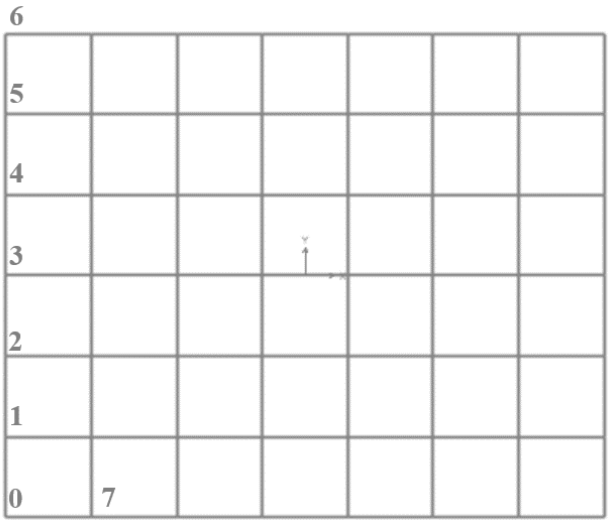

Figure 13. Numerating the columns on an example floor plan

Table 7. Example summary of column positions and stiffness contributions in both axes

Number of Column	X Coordinate (m)	Y Coordinate (m)	Member Height in X	Member Height in Y	Kx (Hx*Xcoord)	Ky (Hx*Xcoord)
0	0.0	0.0	0.5	0.5	0.0	0.0
1	0.0	3.0	0.5	0.5	0.0	1.5
2	0.0	6.0	0.5	0.5	0.0	3.0
3	0.0	9.0	0.5	0.5	0.0	4.5
4	0.0	12.0	0.5	0.5	0.0	6.0
5	0.0	15.0	0.5	0.5	0.0	7.5
6	0.0	18.0	0.5	0.5	0.0	9.0
7	3.0	0.0	0.5	0.5	1.5	0.0

Then, by dividing the total stiffness by the total column heights in both directions, the coordinates of the original position of the center of rigidity are calculated. Since every column has been placed symmetrically, the center of rigidity is in the centroid of the floor plan (Figure 14).

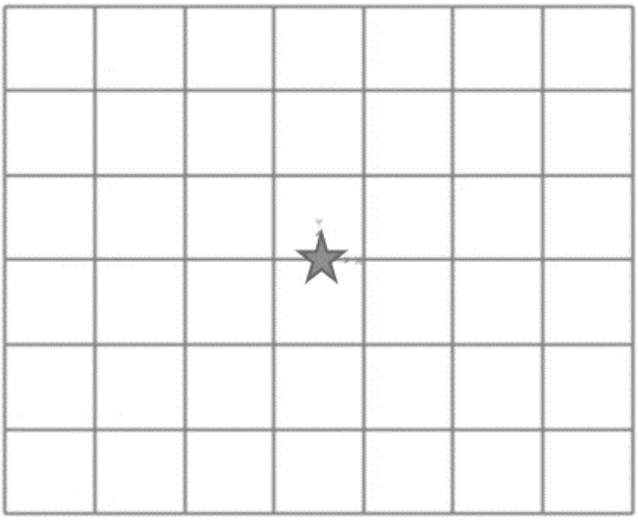

Figure 14. The original position of the centroid in the example floor plan

After finding the original position, the written code starts to make trials to achieve the input eccentricity ratio or greater. The code sets boundary lines for both horizontal axes starting from one corner in each step until it satisfies the eccentricity limit (Figure 15).

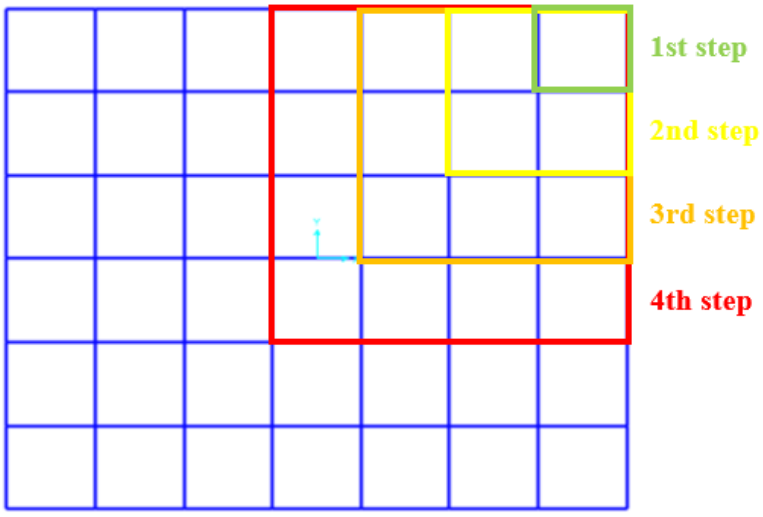

Figure 15. Iteration steps to achieve the input eccentricity on the example floor plan

After iterations, the code solves in the 3rd step by deleting 9 columns in the upper right corner as (Figure 16)

$$CR_{org} = (10.5, 9.5)\ m \qquad (7X, 6Y \;\; dx = dy = 3\ m)$$
$$CR_{new} = (9.06, 7.85)\ m \qquad ecc = (13.68\%, 12.77\%)$$

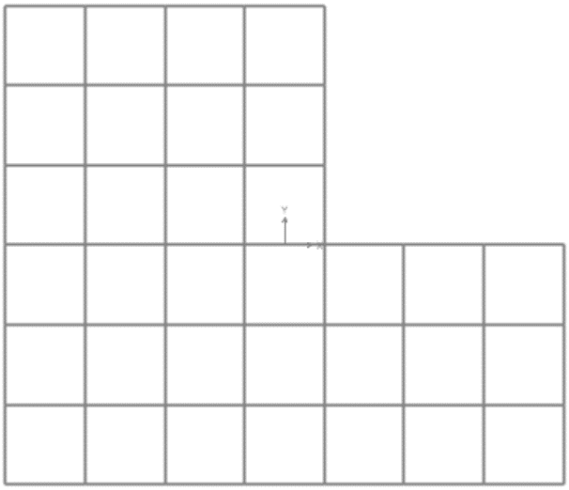

Figure 16. The example floor plan with the plan irregularity application

The code tries to achieve the eccentricity goal up to a minimum number of spans to maintain framing in the critical direction. In the example case, the y direction has a smaller number of spans.

If the structural system possesses shear walls, the column table represented previously is modified respectively to height and coordinates. Then the same procedure is applied once again.

2.3.2.4 Vertical Irregularity

Since the short column and soft story irregularities are already reflected in the model, many attempts have been made to define an extra vertical irregularity. Vertical irregularity condition was first implemented by increasing the story height by 50% for the third and last stories. Then, column discontinuity in inner frames, which is one of the most observed vertical irregularity types in real practice, is implemented. First, a reference frame with 4x3 bays is generated. Then all the following conditions are realized one by one to observe the effect of vertical irregularity on the response of the structural model:

- Height modification,
    - the height of the last and the third story is increased by 50%, which results in a reduction in stiffness.
- Deleting four of the inner columns in the center of the floor plan,
    - Four of the inner columns are deleted together with the height modification to observe the effect (Figure 17).

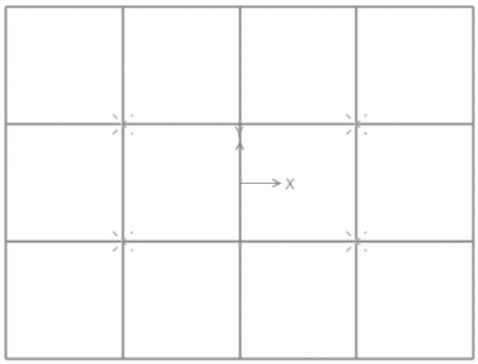

Figure 17. Selected four inner columns to be deleted in the reference frame floor plan

- Symmetrically deleting two of the inner columns in the center of the floor plan,
    - Two of the inner columns are deleted symmetrically together with the height modification to observe the effect (Figure 18).

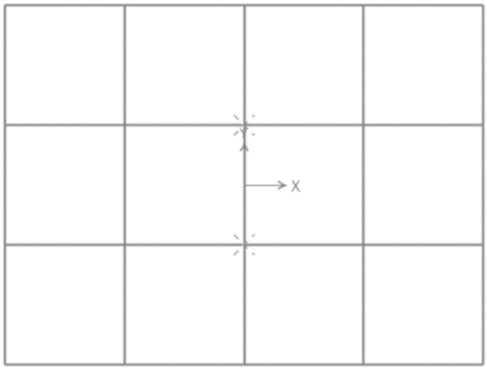

Figure 18. Selected symmetrical two inner columns to be deleted in the reference frame floor plan

- Asymmetrically deleting two of the inner columns in the center of the floor plan,
    - Two of the inner columns are deleted symmetrically together with the height modification to observe the effect (Figure 19).

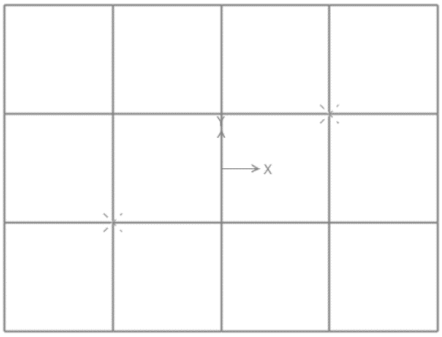

Figure 19. Selected asymmetrical two inner columns to be deleted in the reference frame floor plan

The pushover curves for all considered cases are demonstrated in Figure 20 together with the reference case. All of the cases to simulate vertical irregularity exhibit similar reductions in base shear strength whereas the displacement capacity and displacement-based limit states do not seem to differ significantly.

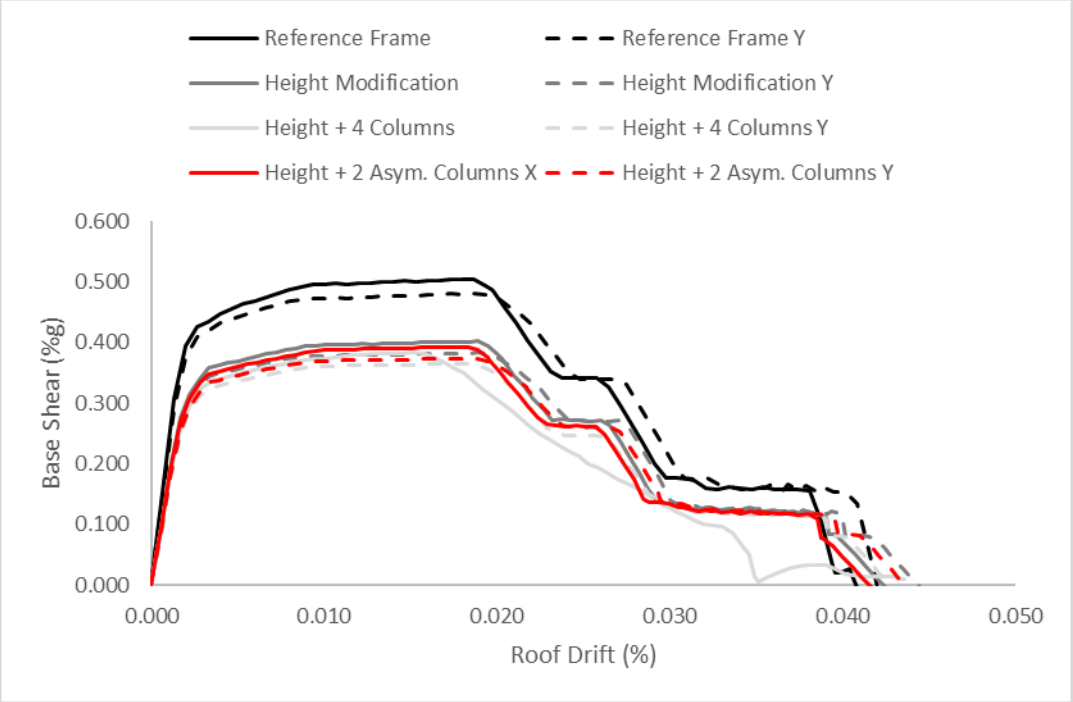

Figure 20. Comparison of the pushover response of each possibility

As can be seen from Figure 20, deleting the inner columns could not create any significant effect on the reference frame. Therefore, only height modification was decided to be kept representing the stiffness reduction due to vertical irregularity in this study.

2.3.2.5 Short Column

Short (or captive) column conditions generally occur on the ground floor. To represent this effect, the heights of edge columns of the first floor are reduced to 1/3 of the original height of a column.

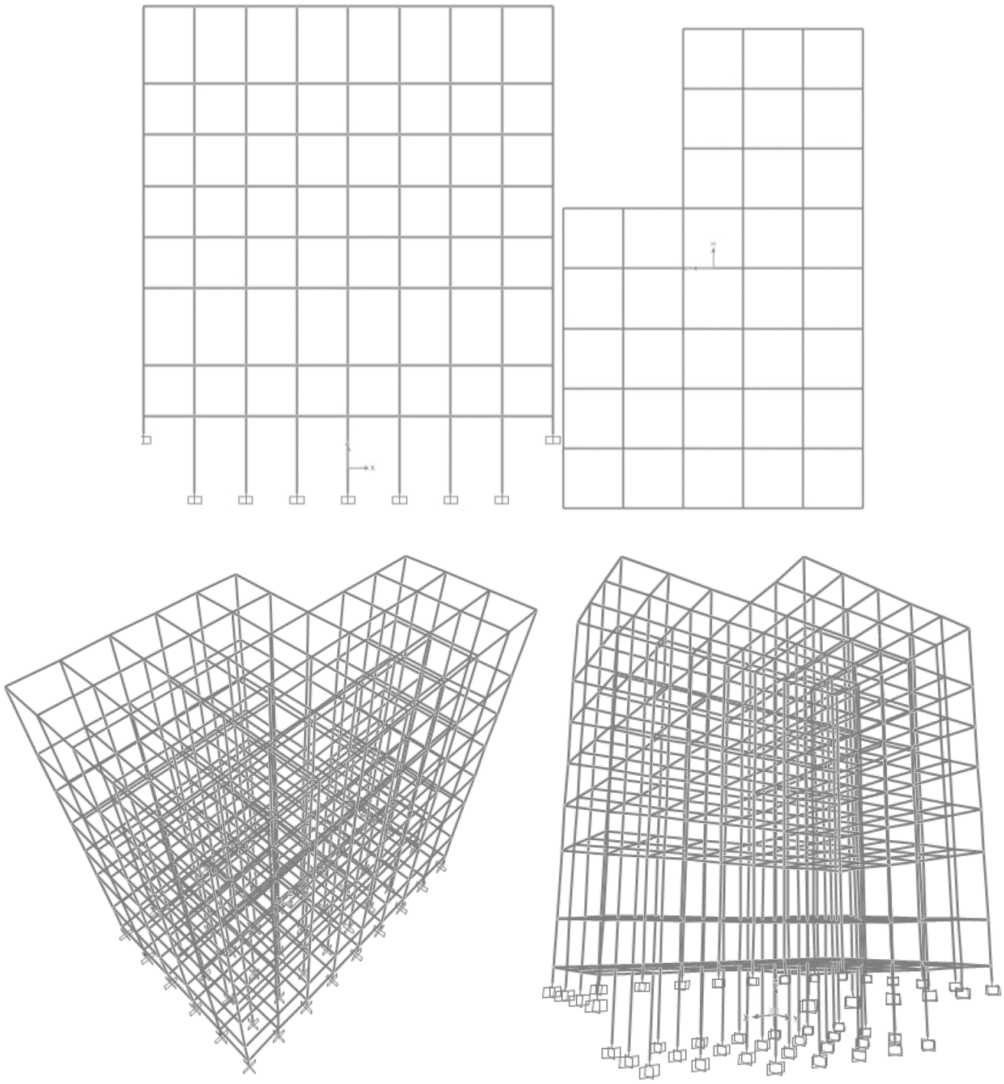

Figure 21. Representation of all structural irregularities in an example 3D model

2.3.3 Sensitivity of Structural Parameters

To observe the sensitivity of all parameters affecting the structural modal one by one, a reference 3D frame was generated with the following properties as seen in Table 8.

Table 8. Summary of structural parameters of the reference frame

Name of the variable	Unit	Value of the variable
Number of stories	-	5
Construction year	-	2020
Usage class	-	Residential
Cantilever ratio	Percent	0
Soft story	Boolean	False
Short column	Boolean	False
Plan irregularity	Percent	0
Vertical irregularity	Boolean	False
Shear wall ratio	Percent	0
Concrete strength	MPa	30
Reinforcement strength	MPa	420
Beam reinforcement ratio	Percent	1.0
Column reinforcement ratio	Percent	1.5
Number of spans in each direction	-	3
Span lengths in each direction	Meters	3
Story height	Meters	3
Beam cross-sections	Centimeters	25 x 40
Column cross-sections	Centimeters	50 x 50
Slab thickness	Centimeters	10

Then the structural model has been subjected to the application of each variable, including structural peculiarities, individually. To compare the capacity curves in terms of base shear capacity and drift capacity, pushover analyses were performed in both horizontal directions.

2.3.3.1 Effect of Construction Year

The reference frame has been updated by taking into account all considered seismic codes and the year of construction. In particular, the years 1975, 1998, 2007, and 2018 have been considered. With less code compliance, the base shear capacity of the model has been drastically lowered (Figure 22). However, the capacity curves for the structures designed following TEC1998 and TEC2007 are remarkably similar. This is due to the fact the related regulations in these codes do not differ significantly. Instead of the design of new structures, performance limitations for existing structures have been the most important enhancement in the 2007 seismic code.

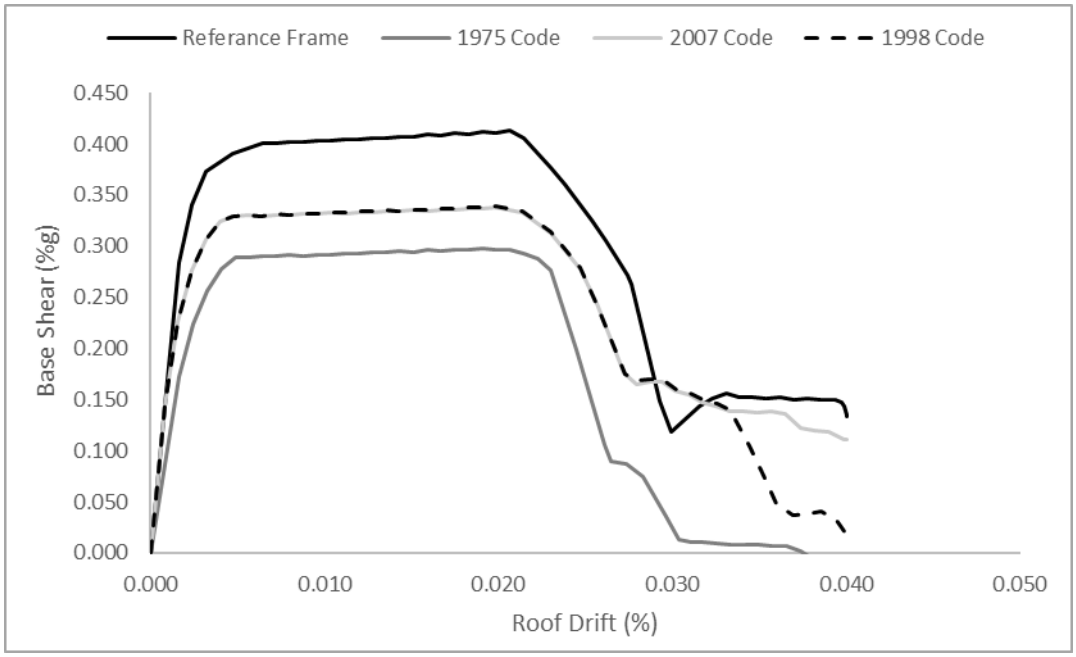

Figure 22. Comparison of the capacity curves of older buildings with the reference frame

2.3.3.2 Effect of Occupancy Type

Figure 23 compares the residential and non-residential occupancy types. The live load applied to the floor slabs and the live load participation factors in the dynamic analysis are the two main differences between these two capacity curves. Non-residential structures participate in structural loads significantly more than residential buildings, but they are nonetheless equally stiff relative to the reference frame. As a result, shear force capacity is severely reduced as anticipated.

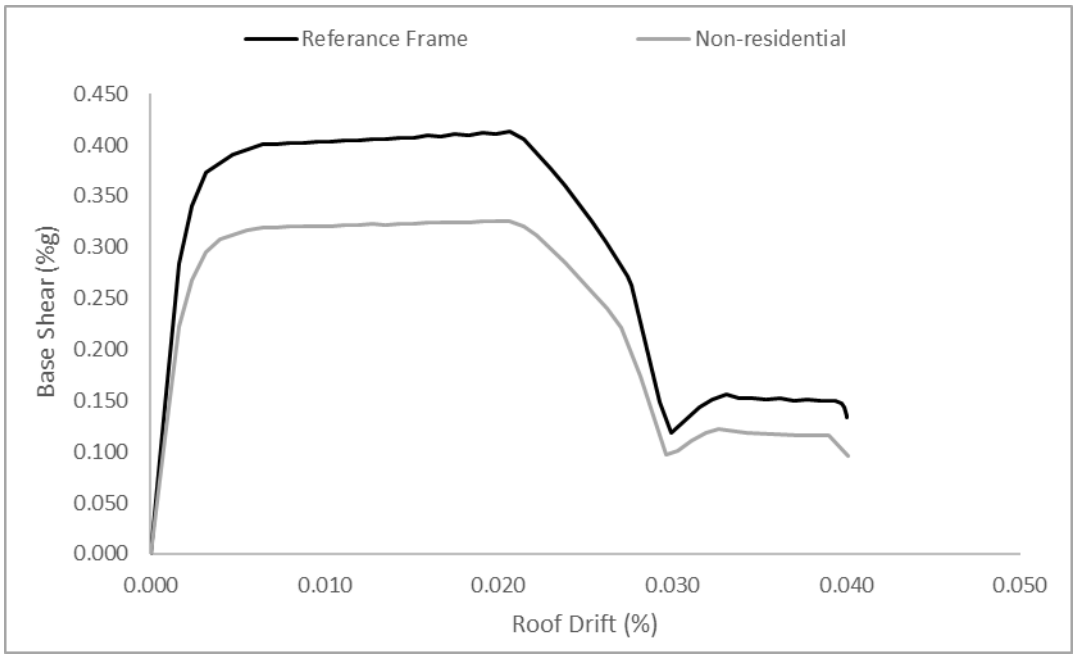

Figure 23. Comparison of the capacity curves of non-residential buildings with the reference frame

2.3.3.3 Effect of Heavy Cantilevers

After the reference frame is modified by a cantilever ratio of 30%, which results in 2.7 m long cantilevers in both axes, the base shear capacity of the structural model is significantly reduced (Figure 24). This may be because cantilevers add a large amount of mass to the structure without increasing the system's overall stiffness. The result is comparable to the difference encountered in the case of occupancy type comparison.

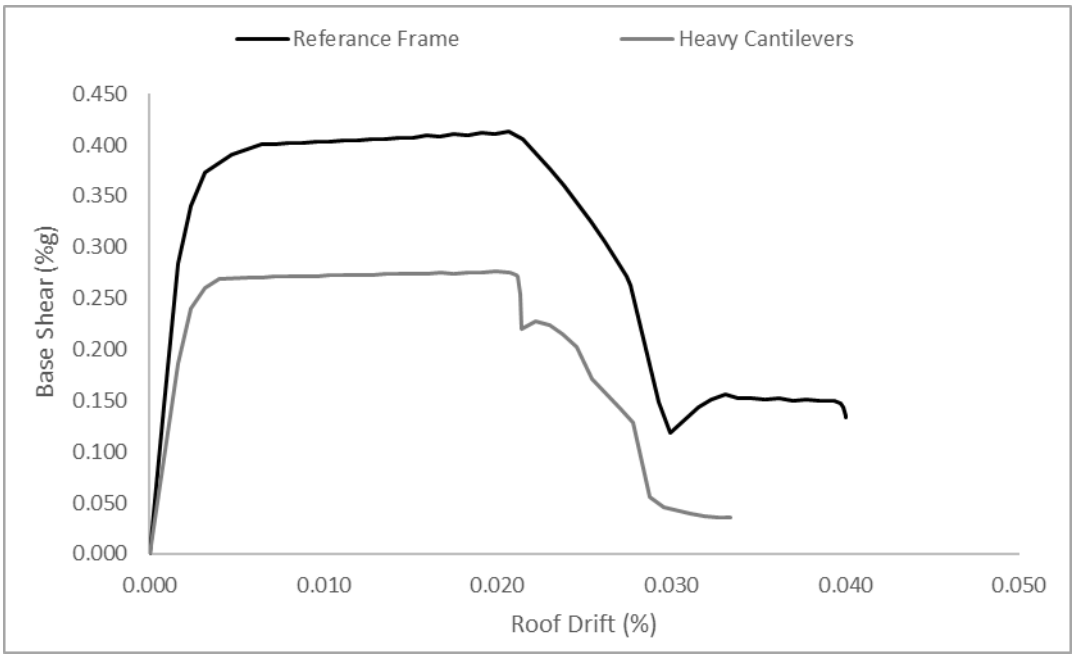

Figure 24. Comparison of the capacity curves of the building having heavy cantilevers with the reference frame

2.3.3.4 Effect of Soft Story

Under the influence of lateral loads, the ground story columns often experience the most essential capacity utilization. In soft story irregularity, the story height of the ground floor is increased by 50%, significantly reducing the stiffness of the system as a whole. The capacity comparison with the reference frame makes it simple to observe this behavior (Figure 25).

Figure 25. Comparison of the capacity curves of the building having a soft story irregularity with the reference frame

2.3.3.5 Effect of Short Column

The inclusion of short columns has revealed the most significant effect in this parametric study (Figure 26). This is because the short column formation results in a considerably more brittle shear failure than the anticipated ductile bending failure in the columns of the structure. The structure can not even reach the yield state, as shown in Figure 26, and it suddenly fails without any inelastic deformation.

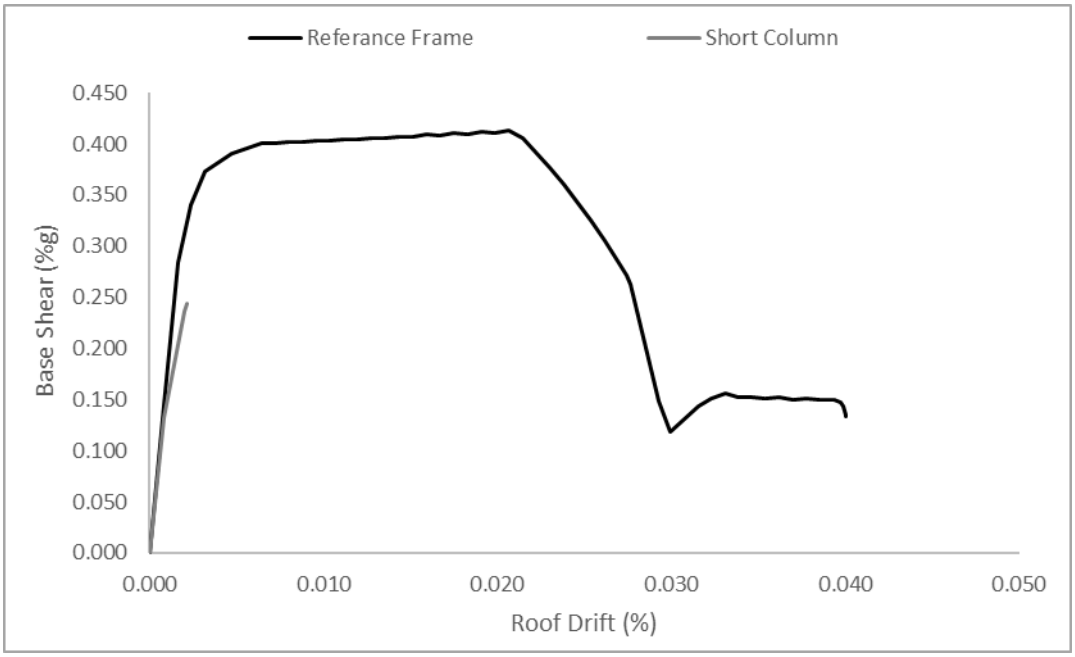

Figure 26. Comparison of the capacity curves of the building having a short column deficiency with the reference frame

2.3.3.6 Effect of Plan Irregularity

Plan irregularity causes eccentricity in the system by moving the center of rigidity away from the system's center of mass. It should be noted that the vertical elements at the corners are removed from the floor plan to illustrate this irregularity. As can be seen in Figure 27, this parameter has no impact on the base shear capacity since it simultaneously reduces the mass and stiffness of the system. The building's ability to withstand lateral deformation is reduced, nevertheless, as a result of torsional effects.

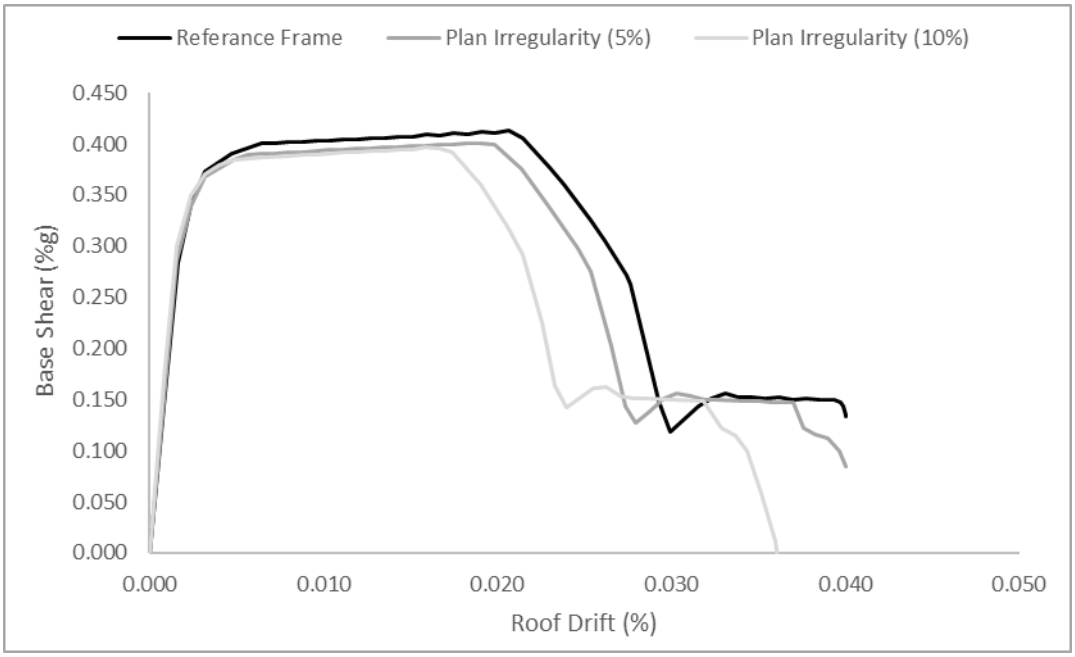

Figure 27. Comparison of the capacity curves of the building having different percentages of plan irregularity with the reference frame

2.3.3.7 Effect of Vertical Irregularity

The story height at the third and last floors is increased by 50% in vertical irregularity, which significantly reduces the stiffness of the system as a whole (Figure 28). The capacity comparison with the reference frame makes it simple to observe this behavior. The soft story irregularity has a very similar impact.

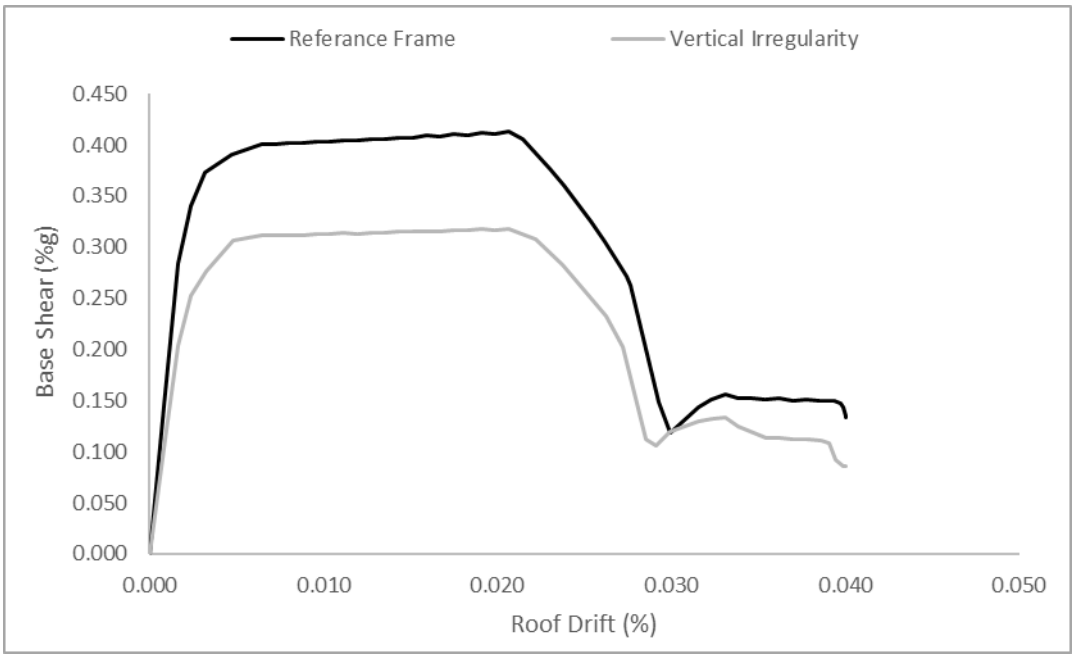

Figure 28. Comparison of the capacity curves of the building having vertical irregularity with the reference frame

2.3.3.8 Effect of Shear Walls

Without significantly increasing the dead load, shear walls significantly increase the lateral stiffness of the system. As a result, the system's period of vibration is decreased. The impacts of various shear wall area ratios are compared concerning the reference frame in Figure 29. The use of a 2% shear wall within the frame approximately doubles the base shear capacity. However, there is a trade-off between the load-carrying capacity and the lateral deformation capacity, which is nearly halved, because it decreases the ductility of the system.

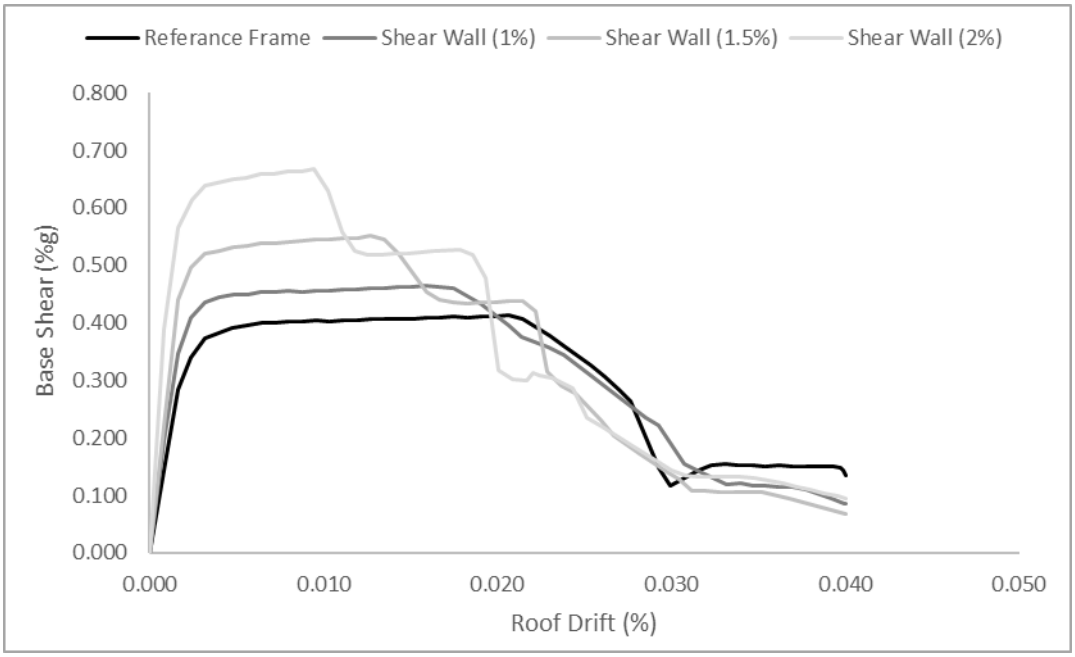

Figure 29. Comparison of the capacity curves of the building having different amounts of shear wall areas with the reference frame

2.3.3.9 Effect of the Change in Strength of Concrete

With the lowered concrete grade, mechanical characteristics like concrete compression strength and modulus of elasticity are altered. The difference can be essentially insignificant, as shown in Figure 30. In an actual building, however, it will have a far more detrimental effect because the ductility ratio delivered by the same amount of reinforcement is directly proportional to the concrete capacity. However, since only the concrete contribution is measured in this example by maintaining constant reinforcement properties, it is apparent why the influence on the building is so minimal.

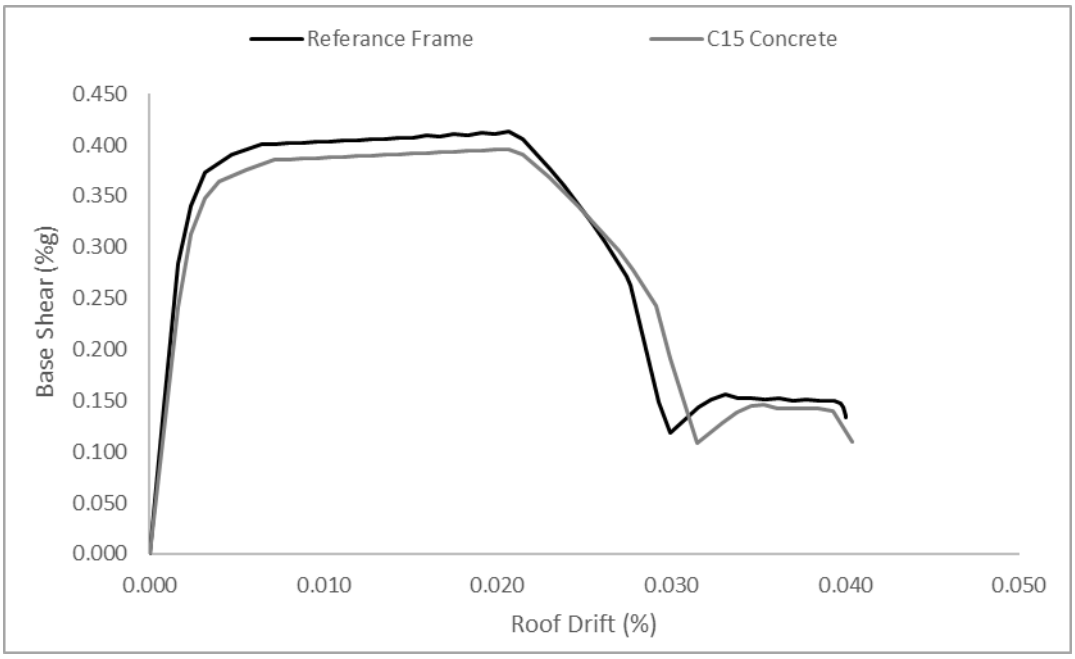

Figure 30. Comparison of the capacity curves of the building having a lower concrete grade with the reference frame

2.3.3.10 Effect of Change in Strength of Steel Reinforcement Bars

When the steel grade is reduced, mechanical characteristics like compression strength and modulus of elasticity are altered. The upper limits of the building's capacity are forced in the static pushover analysis (Figure 31). The yield capacity of the employed reinforcing steel may be the most crucial factor for an RC structure for upper limit states. As anticipated, a significant reduction in the building's base shear capacity is observed when the yield strength is reduced almost to half.

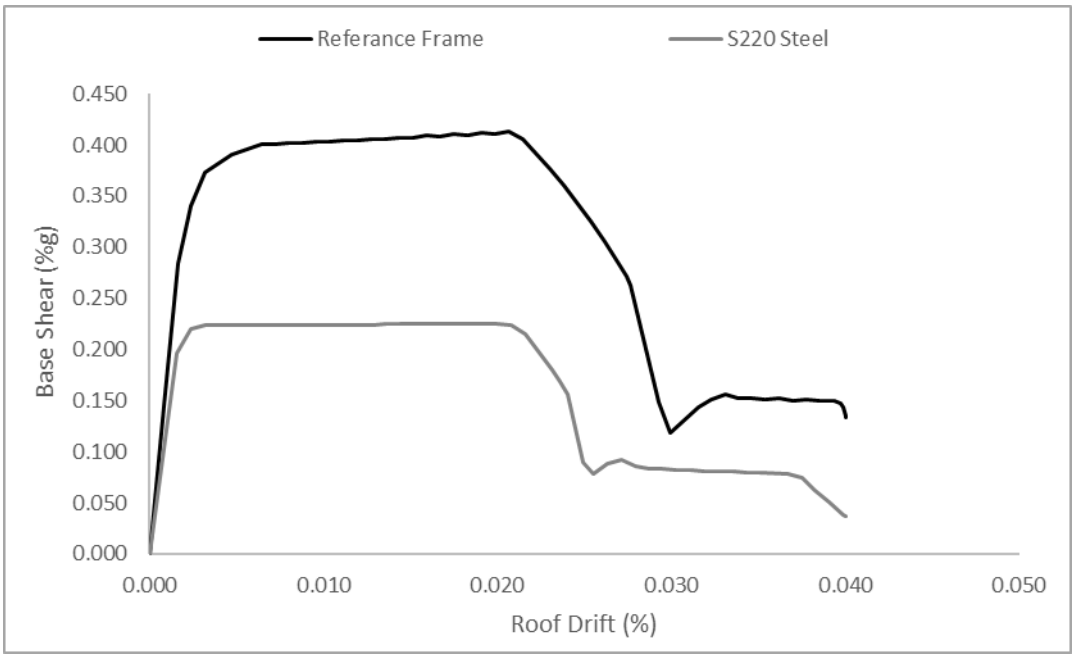

Figure 31. Comparison of the capacity curves of the building having a lower steel grade with the reference frame

2.3.3.11 Effect of Using a Higher Reinforcement Ratio

Contrary to the code-checked ratios in the reference building, the reinforcement ratio is favored as 2% for beams and 4% for columns, which is defined as the maximum ratio under the TS-500 rules. The base shear capacity of the building seems to have increased by more than double, as can be seen in Figure 32.

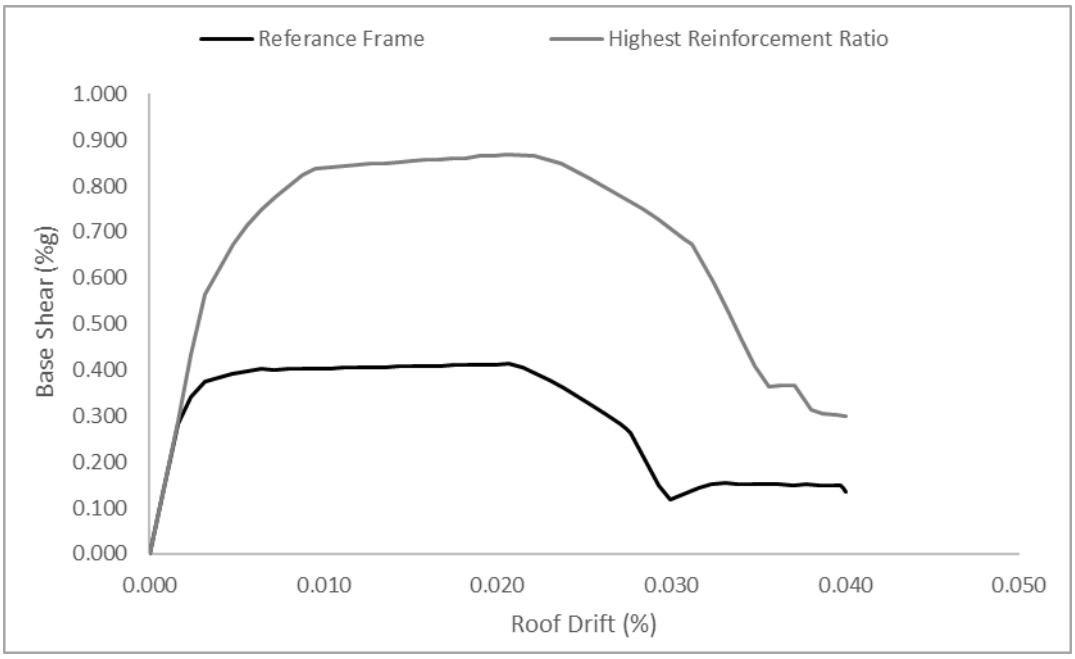

Figure 32. Comparison of the capacity curves of the building having higher reinforcement ratios with the reference frame

2.3.3.12 Effect of Change in Cross-Section Dimensions of Beams and Columns

Despite the reference building having 50 x 50 cm columns, the sample case utilized in this comparison employed 30 x 30 cm column dimensions, which is the minimum requirement in the TBEC-2018. As a result of the significant reduction in the lateral stiffness of the building, the base shear capacity declined as anticipated (Figure 33).

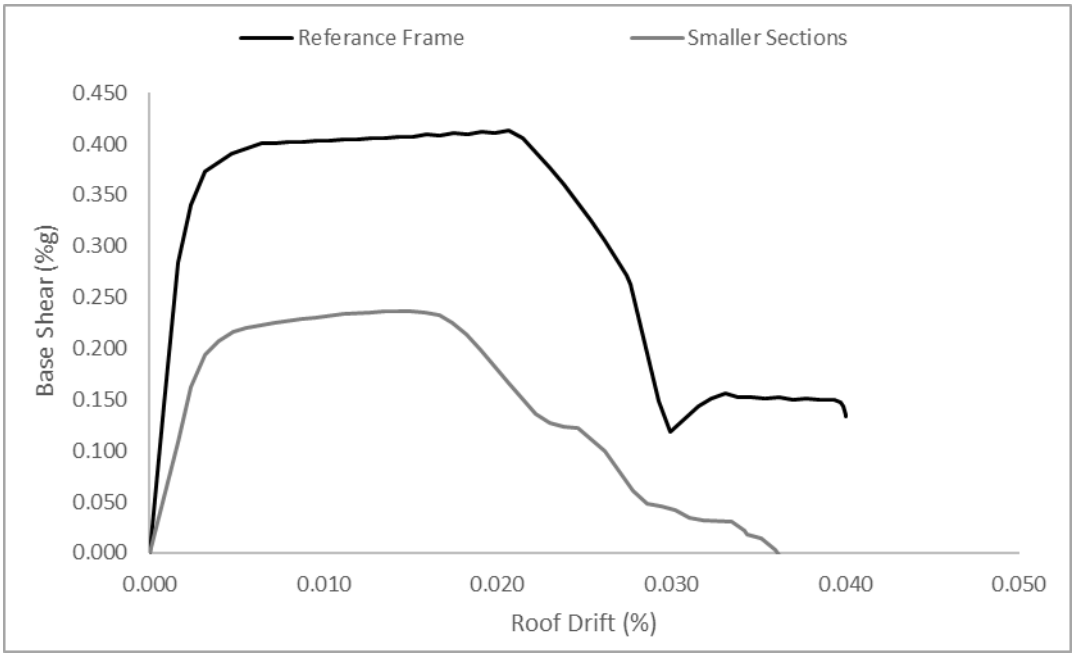

Figure 33. Comparison of the capacity curves of the building having smaller structural members with the reference frame

2.4 Concluding Remarks

This section of the thesis discusses how computer models are created in general terms. First, the parameters influencing the dynamic behavior of the building under earthquake excitation are discussed. The characteristic distributions of these factors in Turkiye's building stock were then determined by referring to statistical investigations conducted in different regions of our country. Furthermore, the sampling preferences utilized while developing building models are presented. Following that, it was discussed how these parameters were represented in computer models, and a sensitivity study was carried out to explore the effects of variations in these parameters.

To summarize, the input parameters to the models were the number of stories (1-12), construction year (1975-2023), occupancy class (residential or non-residential), structural irregularities (soft story, short column, heavy overhangs, plan, and vertical irregularities), whether there is a shear wall in the structural system, material, and geometric features.

All parameters of a building considered, except its material and geometric properties, determine which building subclass the building falls into. As a result of different realizations created by considering the number of stories, the last 4 earthquake regulations in our country, occupancy class and different combinations of structural irregularities, a total of 4768 building subclasses have emerged. Then, it was decided to create 20 samples to find the average behavior of each subclass. This means that a total of 95360 different building models should have been created.

That is why a fully automated technique was devised with the Python programming language by utilizing the SAP2000 application programming interface. A building model can be created from scratch based on the supplied specifications and the results of linear and nonlinear analyses were summarized.

CHAPTER 3

CAPACITY CURVE GENERATION FOR BUILDING MODELS

3.1 Analysis Stage and Gathering the Results

As stated in Chapter 2, after accounting for the building's structural irregularities, occupancy class, year of construction, and number of stories, 4768 RC structure subclasses were found. Using the SAP2000 analysis software, a total of 95360 structural models were created by creating 20 samples for each building subclass. Then, for every numerical model, nonlinear static pushover analyses are performed for each perpendicular direction.

It was determined that only the data needed for this, and future investigations should be retained, as keeping all files containing model output would necessitate a significant amount of storage space and decrease computational efficiency. In this case, the results of the modal analysis, including modal periods, mode shapes, and modal mass participation, are stored in the model setup file with the extension "$2k," which makes it simple to recreate the model if needed. Lastly, the results of the static pushover analysis in two perpendicular directions are stored.

In the computer lab located in the Middle East Technical University Civil Engineering K1 Block Main Building, analyses were achieved by running 20 machines simultaneously. Then, all the results obtained from the computer outputs were stored and analyzed in detail.

3.2 Idealization (Linearization) of the Capacity Curves

Following the investigation, the findings of the continuous and erratic static pushover analyses were simplified and idealized by considering the guidelines outlined in FEMA356 (2000) and ASCE 41-17 (2017).

According to FEMA356 (2000), to compute the building's effective lateral stiffness, K_e, and effective yield strength, V_y, an idealized relationship for base shear and control node displacement replaces the nonlinear force-displacement relationship. This relationship has a post-yield slope with parameter α and an initial slope of K_e. It has a bilinear form. A graphical method that iteratively balances the area above and below the curve is employed to locate line segments on the idealized force-displacement curve. The secant stiffness computed at a base shear force equivalent to 60% of the structure's effective yield strength is the effective lateral stiffness or K_e.

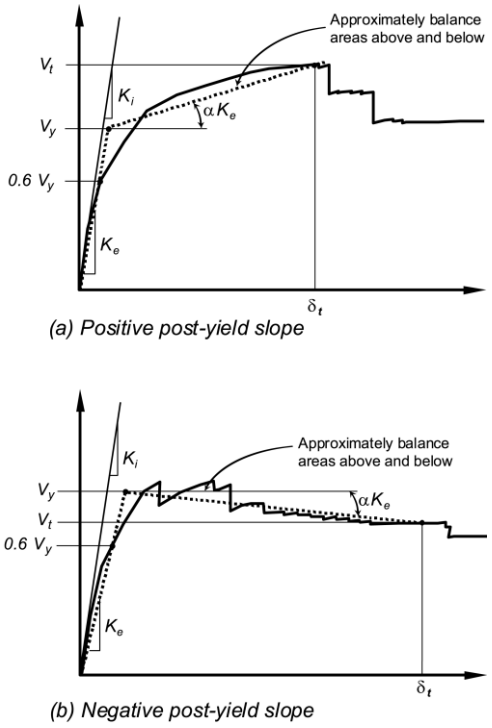

Figure 34. Idealized force-displacement curves according to FEMA356 (2000)

According to ASCE 41-17 (2017), the procedure for fitting the first bilinear part is defined in the same way as represented in FEMA356 (2000). Additionally, it also defines the slope after the capping point as the point at which the base shear decreases to 60% of the effective yield strength and the end of the positive post-yield slope (V_d, Δ_d) determines the negative post-yield slope (α_2Ke), which will be represented by the third line segment.

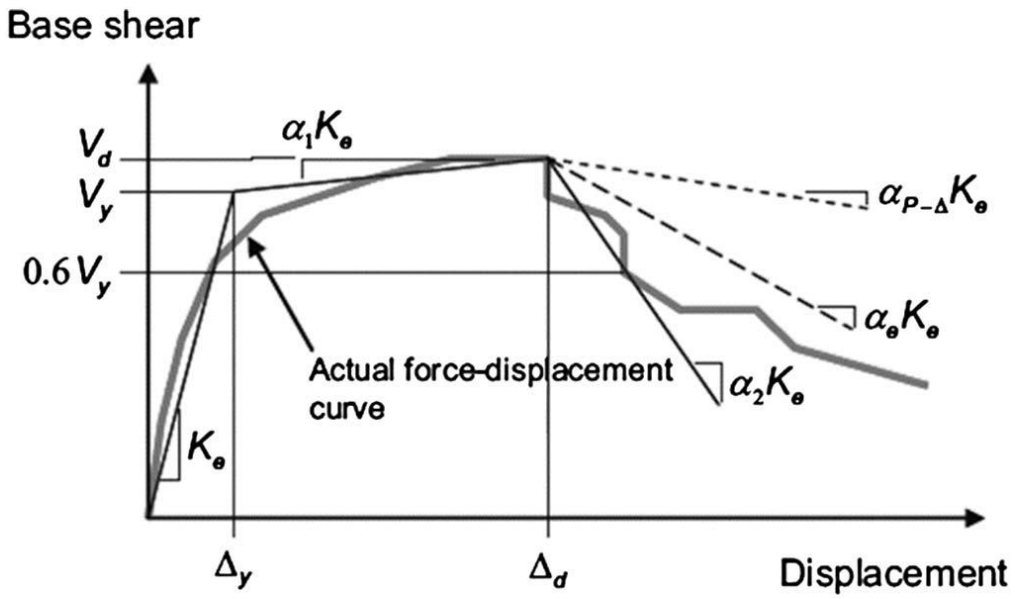

Figure 35. Idealized force-displacement curves according to ASCE41-17 (2017)

According to the nonlinear static procedure results obtained from the numerical models, base shear values were calculated up to 60% or below the yield force capacity shown by ASCE41-17 (2017) in some cases. Example capacity curves for this case are presented in Figure 36.

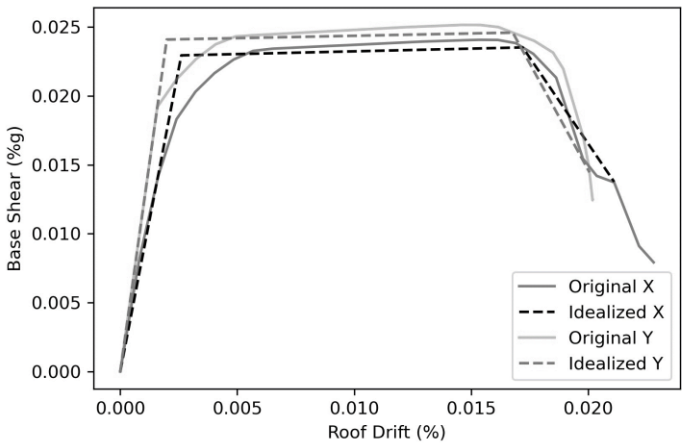

Figure 36. An example of trilinearization for pushover curves of an 8-story building by ASCE 41-17 (2017)

In some cases, the pushover analysis does not contain a descending branch after the capping strength capacity. In the case of such models, using a bilinear fit rather than a trilinear fit can be preferred. Accordingly, it becomes unable to identify the parameter corresponding to the stiffness drop beyond the capping point. The following figure shows an example capacity curve for this specific case.

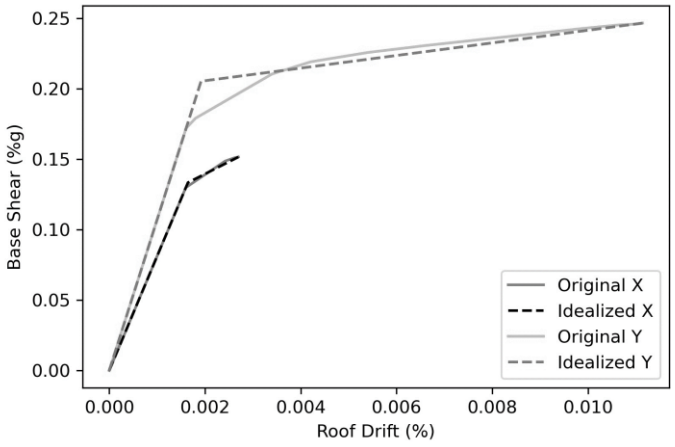

Figure 37. An example case of bilinearization for the pushover curve of a 10-story building

There are also such cases in which, the pushover curves of some numerical models failed without showing any plastic behavior, that is, without having any ductility value. In such cases, linear fit has been preferred instead of bilinear fit. For this reason, only the base shear force coefficient and elastic stiffness values of the model could be obtained. Figure 38 shows an example capacity curve for this specific case.

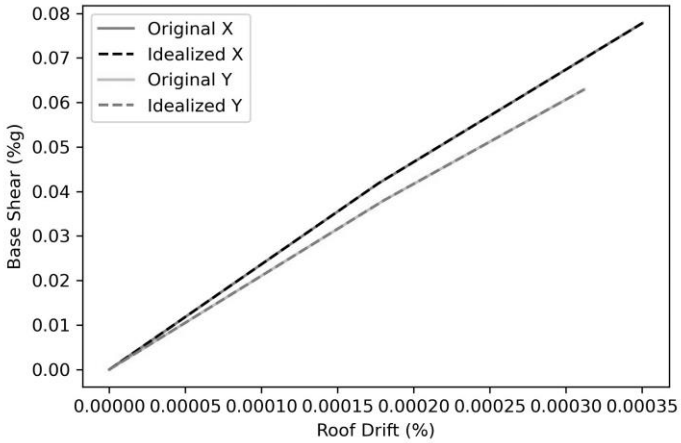

Figure 38. An example linearization for the pushover curve of a 10-story building

3.3 Possible Utilization of the Capacity Curves

In many structural vulnerability studies available in the literature, the capacity curves acquired within the scope of this thesis study can be used as a reference database in any study that aims to investigate the regional building stock characteristics in Turkiye. In nonlinear time history analyses carried out using idealized SDOF systems—which are usually recommended in the literature—it can be utilized, first and foremost, to define nonlinear hysteretic behavior to the model. The case study carried out in the context of Chapter 4 provides a detailed explanation of this utilization. Furthermore, the Capacity Spectrum Method, which has been widely used in the literature, can also be employed with the idealized capacity curves

acquired. The schematic representation of the steps of both applications is presented in Erberik and Elnashai (2006) as shown in Figure 39.

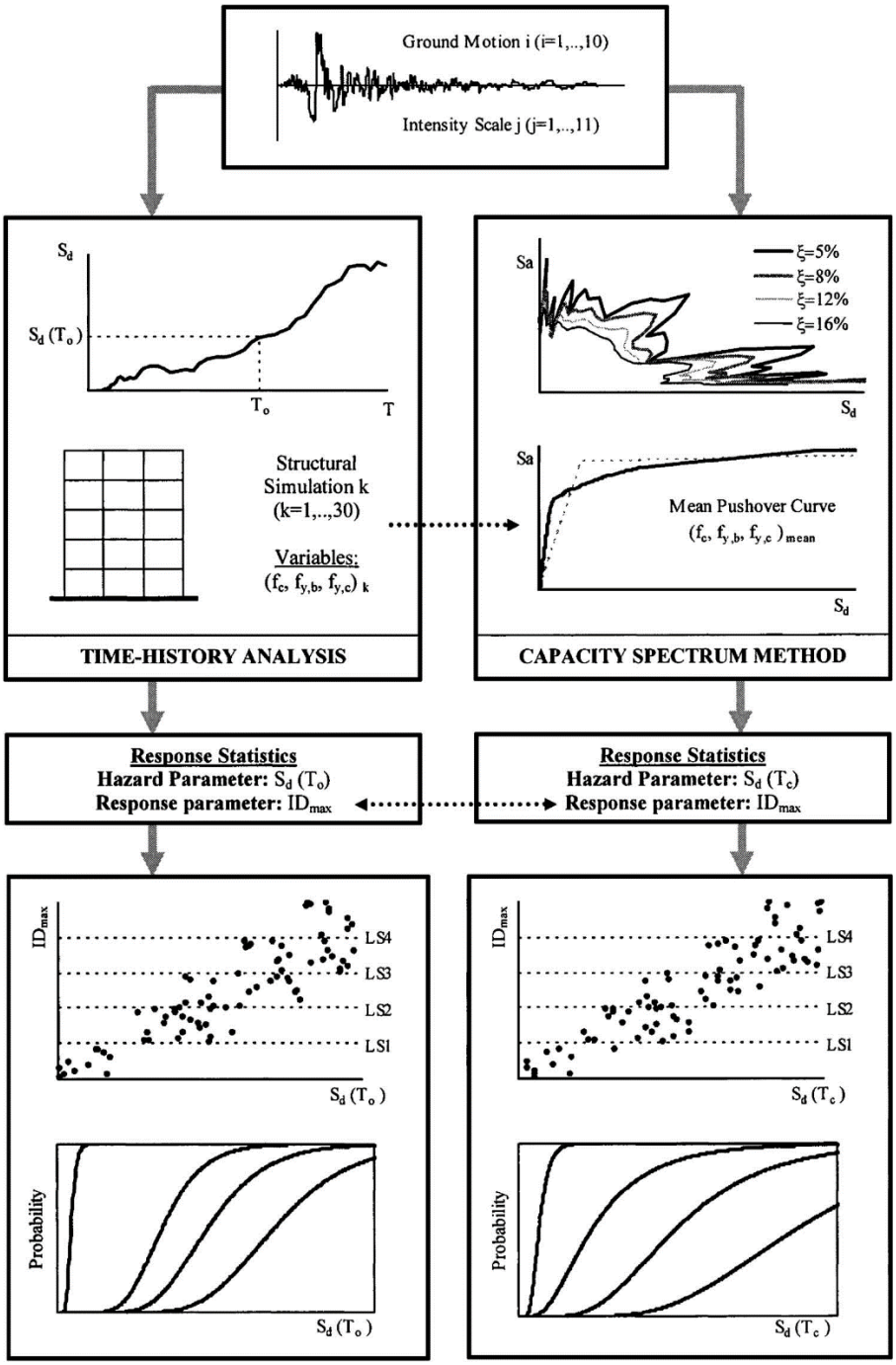

Figure 39. Schematical representation of possible applications of this study (Erberik and Elnashai, 2006)

3.3.1 Capacity Spectrum Method

The Capacity Spectrum Method (CSM), a performance-based seismic analysis technique, can be used for many different purposes, including the rapid assessment of a large population of buildings, design verification for new buildings as they are constructed, seismic evaluation of existing structures to identify damage states, and correlation of damage states of buildings to different ground motion intensities. The CSM compares the structural capacity (shown by a pushover curve) with the corresponding seismic demand (represented by the response spectrum). The performance of the structure is roughly represented by the intersection points of these two curves. Equivalent viscous damping values are applied to linear-elastic response spectra that resemble inelastic response spectra to take into consideration the structural system's non-linear inelastic behavior.

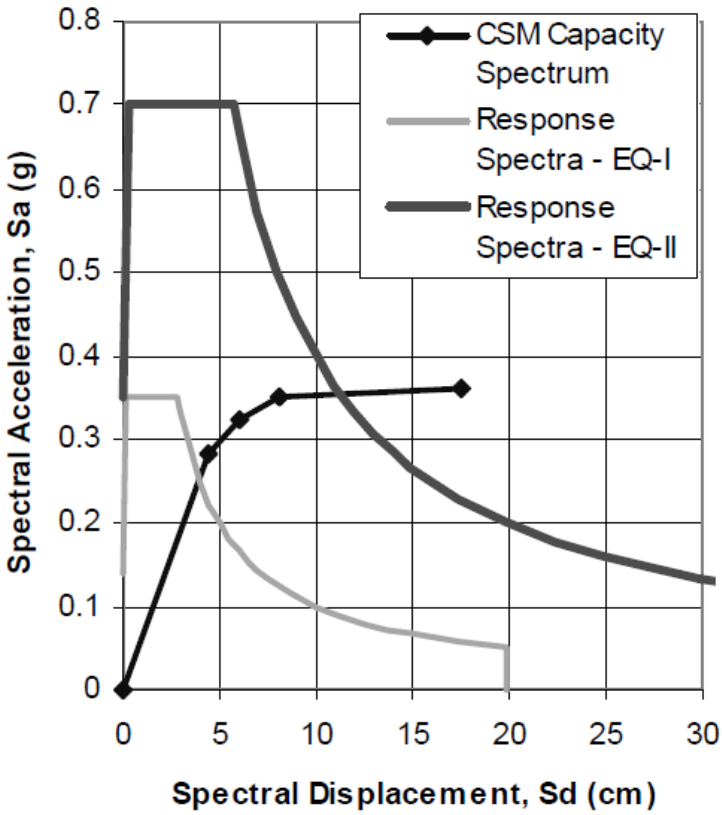

Figure 40. Representation of the CSM (Freeman, 2004)

3.3.2 Dynamic Analysis by using Equivalent SDOF System Idealization

The buildings in the area under consideration can be divided into predefined building classes, and vulnerability data for each class can be obtained using nonlinear time history analyses (NLTHA) and idealized SDOF models that simulate the global response properties of the considered building typology. Given how straightforward the process is, some intrinsic epistemic uncertainty is present in the results, but this is assumed to be acceptable.

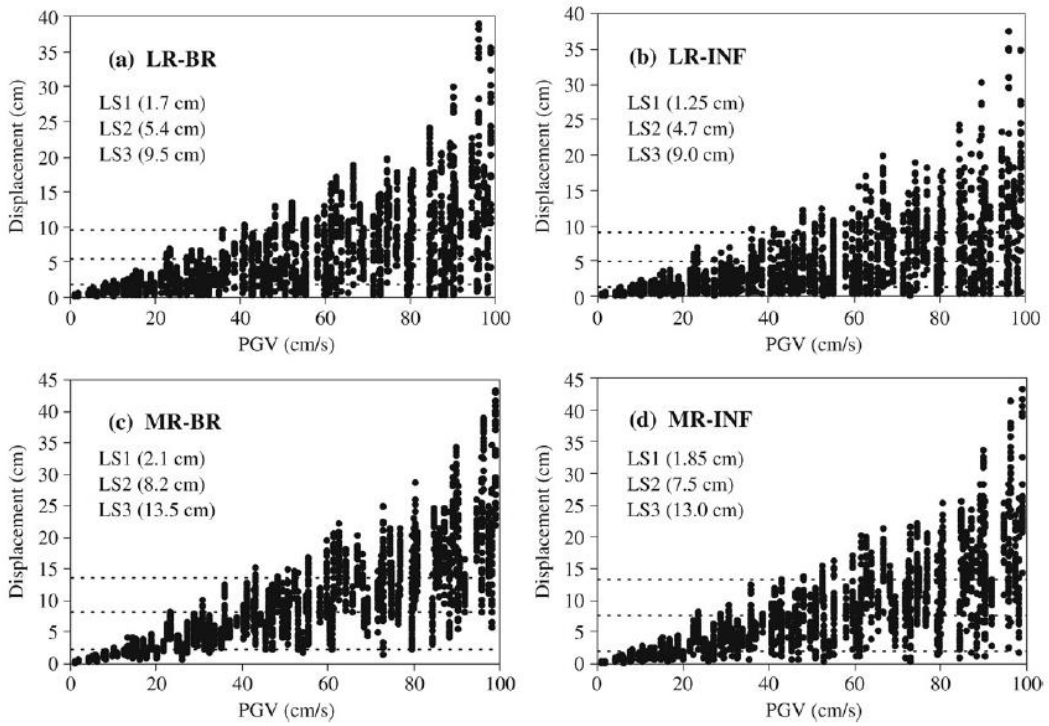

Figure 41. Response statistics from an example study (Erberik, 2008)

3.4 Concluding Remarks

This section of the thesis discusses how the analysis process was completed using the complex input parameters laid out in the previous chapters, and how the obtained results were idealized to create a general perspective on the nonlinear behavior of the building models.

To describe this process in simple terms,

- First, the statistical sampling input parameters are imported into SAP2000.
- All modeling details, such as geometric attributes, loads, reinforcements, diaphragms, plastic hinges, and so on, have been allocated one by one to the structural model.
- Nonlinear analysis for both primary directions begins when the model has been entirely formed.
- Finally, output capacity curves were saved, analyzed, and idealized in a computer environment using the typical processes recommended by ASCE and FEMA356 requirements.

In this way, the key parameters for defining the nonlinear behavior of a building have been obtained, such as fundamental period, force reduction factor, post-yield, and post-capping stiffness ratios. Some images representing this process are shown in Figure 42.

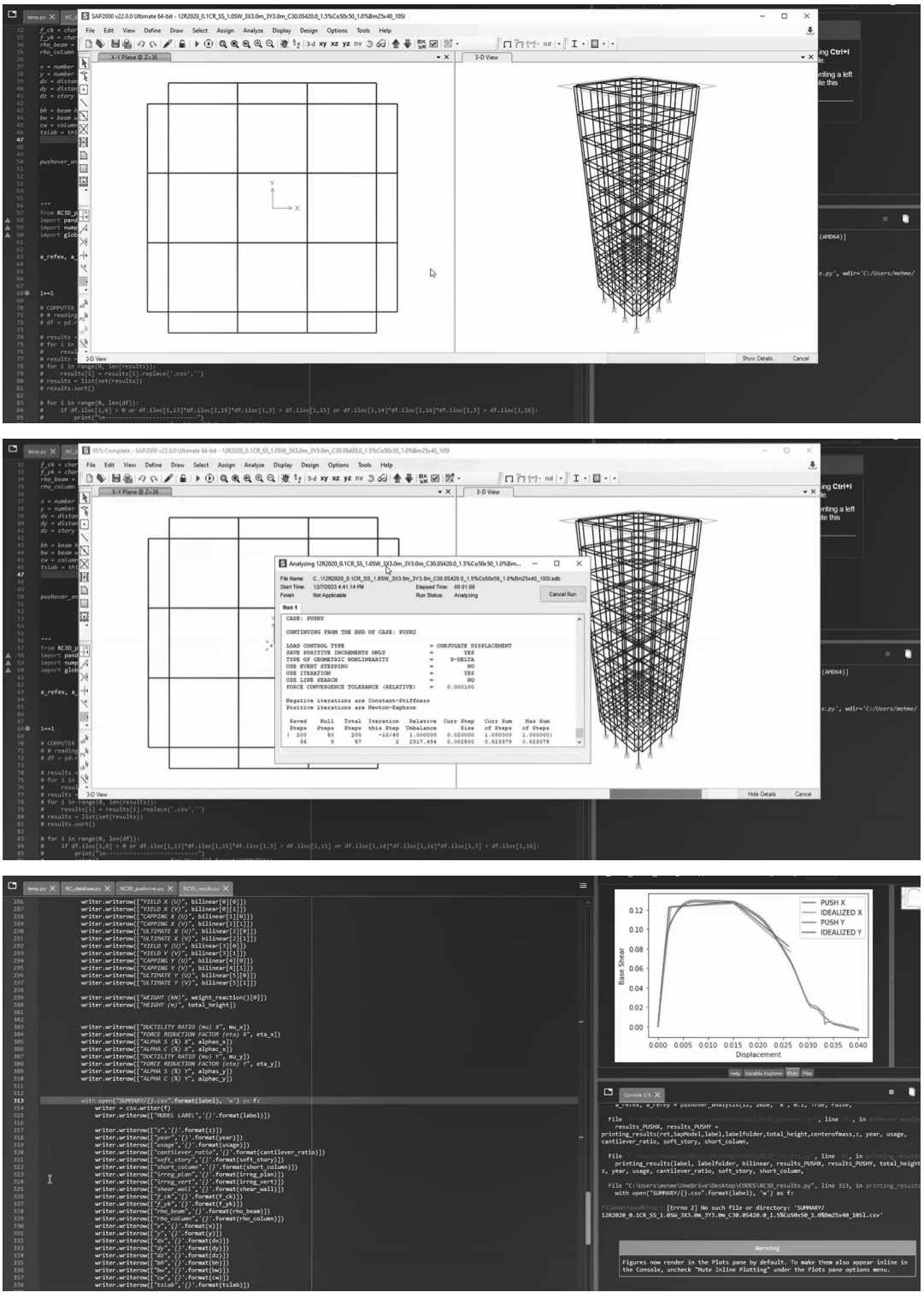

Figure 42. Snapshots from the analysis stage

CHAPTER 4

KAHRAMANMARAŞ/TURKOGLU CASE STUDY

4.1 Introduction to the Conducted Research Project

Turkoglu district of Kahramanmaraş, which is under the influence of Eastern Anatolia and Oludeniz active fault zones, has been studied within the scope of a research project titled "A Methodology for Assessment of Urban Seismic Resilience: Turkoglu, Kahramanmaraş Case Study" funded by National Earthquake Research Program of AFAD, Turkiye under grant number UDAP-C-21-59. The author of this thesis worked as a scholar in this research project, which was carried out between 2021-2023.

The numerical modeling of potential ground motions and intensity distributions for scenario earthquakes based on active faults and regional velocity models was initially conducted in the Turkoglu region of Kahramanmaraş to improve urban seismic resistance. After that, field research was conducted to determine the characteristics of the building stock, and vulnerability data for different building classes was established. In light of these studies, the distribution of estimated seismic damage was obtained during the scenario of earthquakes that had been assumed to occur in the area. Lastly, the orientation of the faults, the site characteristics, the amplitudes and intensities of ground motion, and any potential damages to the building stock were all used as input factors to form the resilience scale that was developed as part of the research project.

4.2 Determination of Structural Vulnerability

As a work package of the aforementioned research project, a building inventory study was carried out in Turkoglu district. The buildings in the district were photographed and some major structural parameters of each building were collected. Then the buildings were classified following the collected data by using some specific criteria. A total of 3700 buildings were evaluated in 6 neighborhoods in the region.

The building statistics obtained from this study followed the ones utilized in previous regional seismic risk assessment studies in Erzincan (Karimzadeh et al., 2018) and Gaziantep (Arslan Kelam et al., 2022) provincial centers. In other words, the building data obtained accurately reflected the features of both urban and rural RC and masonry structures in Turkiye. Then it was decided to apply the building classification scheme that was taken into account for this investigation. For the building stock in the Turkoglu district, 19 distinct building subclasses were identified within the parameters of this classification, which can be seen in Table 9. The last column in the table shows the compliance level of the building class in question with earthquake design principles. Field data is used to establish a parameter for compliance with earthquake design principles. Structures that conform to "high level" earthquake design principles are those that have good visible material quality and no major structural deficiencies (such as soft stories or irregularities in the horizontal and vertical directions). It is anticipated that these kinds of buildings will provide adequate safety in the event of a major earthquake. Conversely, buildings that follow earthquake design principles at a "low level" are those that seem to have substandard construction materials, and deficiencies in structure, and are predicted to perform weakly in the event of a major earthquake. Some structures are expected to perform in between these two limiting cases and they are only partially or moderately compliant with earthquake design standards. To link each RC and masonry building inspected in the field with an earthquake design appropriateness parameter (A/B/C), a scoring system that considers the parameters gathered in the

field has been devised. In light of this procedure, five sub-parameters for RC buildings were considered. Depending on whether the questioned structural deficiencies were present or not, the performance scores shown in Table 10 were applied.

Table 9. Generated building subclasses

Code	Structure Type	Number of Stories	Earthquake Code Compliance
RF1A	RC Frame	1-3	High
RF2A	RC Frame	4-8	High
RF1B	RC Frame	1-3	Moderate
RF2B	RC Frame	4-8	Moderate
RF1C	RC Frame	1-3	Low
RF2C	RC Frame	4-8	Low
RH1A	RC Frame + Walls	1-3	High
RH2A	RC Frame + Walls	4-8	High
RH1B	RC Frame + Walls	1-3	Moderate
RH2B	RC Frame + Walls	4-8	Moderate

Table 10. Scores for subclass scoring of compliance for earthquake design of RC structures

Parameter	Performance Score of the Concrete Structure		
Material Quality	0 (poor)	0.5 (moderate)	1 (good)
Heavy Overhangs	0 (yes)		1 (no)
Soft Story	0 (yes)		1 (no)
Plan Irregularity	0 (yes)		1 (no)
Vertical Irregularity	0 (yes)		1 (no)

The next step was intended to construct representative SDOF structural models and get the structural parameters of these models for each subclass of buildings. A multi-parameter hysteretic model (Ibarra et al., 2005) was utilized in this work to simulate

the global behavior of the pre-existing RC construction subclasses. This model has been evaluated with real data in several scholarly studies (Ibarra and Krawinkler, 2005; Lignos and Krawinkler, 2011; Lignos and Krawinkler, 2012). Additionally, This hysteretic model is available in the material database of OpenSees, an open-source structural analysis platform (McKenna 2011). The input parameters for this hysteretic model, represented in Figure 43a,b, are period, yield capacity, ultimate capacity, ductility ratio, residual strength, maximum displacement, and reduction parameter based on energy consumption capacity.

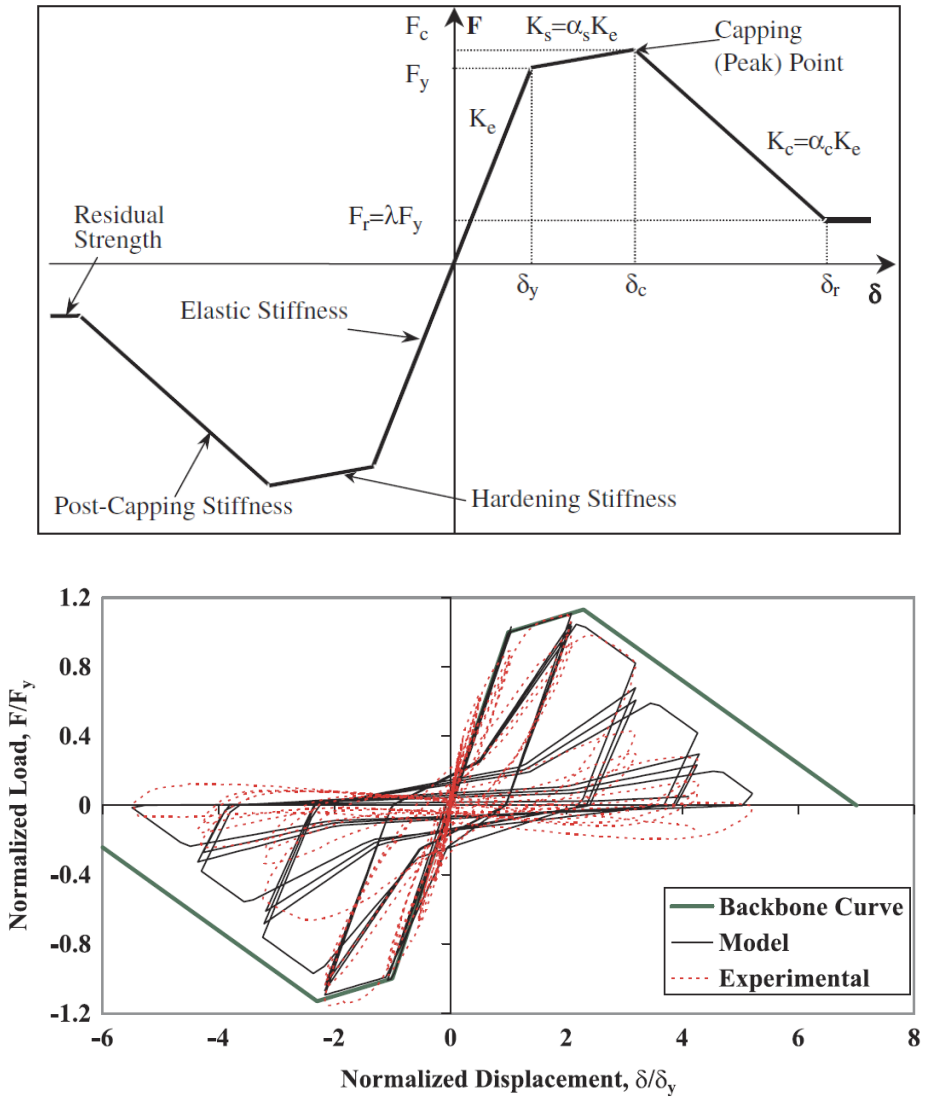

Figure 43. a) capacity curve, b) hysteretic properties of the used hysteretic model (Ibarra et al. 2005)

The aforementioned structural requirements were included in all RC building subclasses and were previously specified in Table 11 (Karimzadeh et al 2018, Arslan Kelam et al 2022). In these studies, the ductility ratio, building period, and ultimate strength capacity—parameters that significantly affect the overall structural performance during an earthquake—were considered random variables. The statistical properties of these random variables (mean and standard deviation) were then ascertained for each building class. The values of the other four parameters were considered constant, depending on the construction subclass in question. Table 11 lists the hysteretic model parameters for each building subclass in the representative models for use in dynamic analysis.

Table 11. Hysteretic model parameters for each RC building subclass

	T (s)		η		μ		α_s (%)	α_c (%)
	MN	**STD**	**MN**	**STD**	**MN**	**STD**		
RF1A	0.38	0.18	0.40	0.08	9.00	3.12	4	-20
RF1B			0.30	0.11	7.30	2.02	4	-25
RF1C			0.23	0.06	4.90	1.47	4	-30
RF2A	0.7	0.27	0.34	0.11	7.10	2.25	4	-20
RF2B			0.26	0.09	6.10	1.75	4	-25
RF2C			0.17	0.06	5.10	1.38	4	-30
RH2A	0.43	0.18	0.59	0.17	4.90	1.40	4	-20
RH2B			0.47	0.13	4.00	1.20	4	-25

When developing idealized models for every RC building class, a sampling approach ought to be employed to acquire structural simulations. The Latin Hypercube sample (LHS) Method, a segmentation-based sample technique that works with many variables, has been employed in this study (Mc Kay et al. 1979). Because the LHS method has a lower computing cost than the Monte Carlo methodology, it has been extensively used in structural earthquake engineering research over the past 20 years. This is because, with a restricted number of samplings, it can yield estimated findings for the intended accuracy level (Erberik and Elnashai 2004, Erberik 2008). Due to these findings, the LHS sampling approach is used in this study to create 20 samples for each random variable. Twenty samples made for 8 distinct building subclasses

for RC buildings were used to produce the models, and 400 synthetic ground motion records that had already been identified were used to run a total of 3200 NLTHAs. The NLTHAs were performed using II-DAP software, which includes the Ibarra-Krawinkler hysteretic model that was previously described (Elkady and Lignos 2019).

In 2020–2021, the first half of the project, three important scenario occurrences were taken into consideration (Figure 44). Since the Amanos (Mw=7.46) and Pazarcik (Mw=7.3) segments are involved in the first occurrence in February 2023, those segments are examined here. To simulate these two occurrences, the stochastic finite fault approach described by Motazedian and Atkinson (2005) is used.

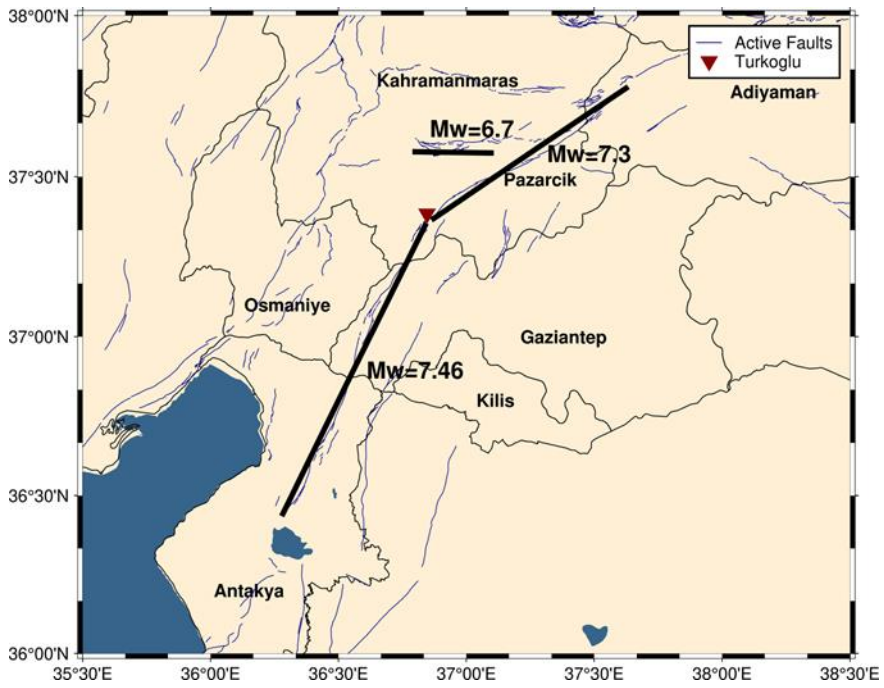

Figure 44. The scenario events considered as part of the AFAD UDAP-C-21-59 project in 2022 (Askan et al., 2022)

In Figure 45, the ground motion models by Boore et al. (2014) and Kale et al. (2015) were compared to the simulated ground motions from the two scenario events for

validation reasons. The comparison was done in terms of PGA, SA (T=0.3 s), and SA (T=1 s). The simulated parameters are found to be usually within ±1 standard deviation of the median values that ground motion models predict. The fact that stochastic ground motion simulations typically estimate the high-frequency content more precisely may be the reason for the minor underestimating of the long-period simulated content. It is also important to note that the datasets used to construct the empirical ground motion models do not contain a substantial amount of data from really large events, such as the Mw7.8 event that occurred on February 6, 2023. It is also observed that the amplitudes from the Amanos scenario are slightly lower, despite their higher magnitude, because of longer source-to-site lengths. These simulated ground motions are employed in the derivation of the fragility curves presented in the next section. High fragility values are to be expected given the high recording intensity, as the comparison results demonstrate.

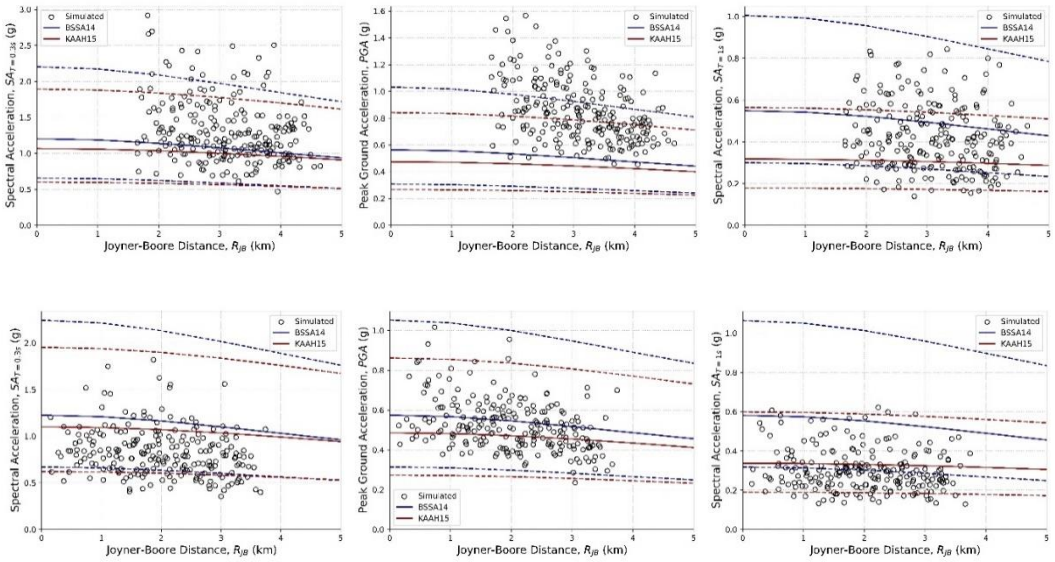

Figure 45. Comparison of simulated ground motions in Turkoglu against empirical ground motion models (top panel: Pazarcik scenario, bottom panel: Amanos scenario) (Askan et al., 2022)

4.3 Derivation of the Fragility Curves

The building simulations display a vertical distribution in terms of the response parameter chosen for various ground motion intensity levels, as may be observed in the sample graphs shown in Figure 46. Peak ground velocity (PGV) is the ground motion parameter and maximum roof displacement (D) is the response parameter chosen in the graph in Figure 46. The response values grow as the ground motion intensity parameter does. By specific definitions and assumptions, the horizontal lines in the chart correspond to predefined damage limit states (LS).

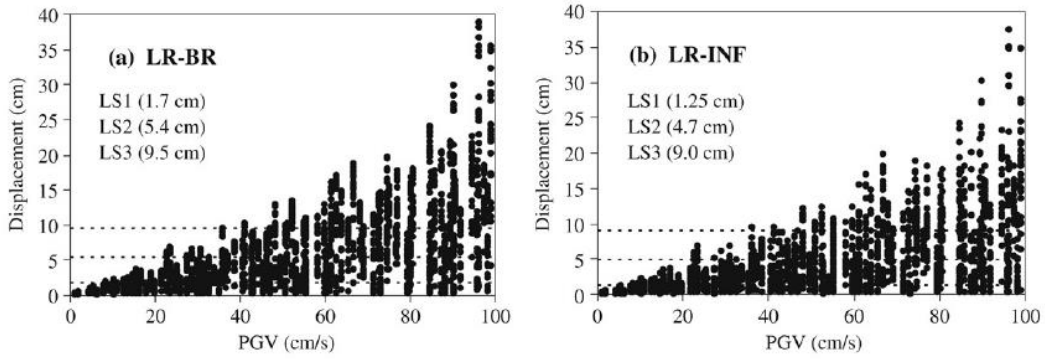

Figure 46. Response statistics from an example study (Erberik, 2008)

It is possible to determine the mean and standard deviation values for each vertical (with a constant intensity measurement value) data group in the figure considering that they satisfy a statistically normal distribution. As a result, each vertical data group in the figure can be described by one of two fundamental statistical description characteristics. Exceedance probabilities for the construction of fragility curves are calculated using these statistical data. The probability of exceedance is the likelihood of going over a damage limit for a particular intensity level. It can be formulated as follows.

$$PE_{i,j} = P\left(RD > LS_i \middle| I_j\right) \tag{4.1}$$

In the above equation, $PE_{i,j}$ representing the exceedance probability of measured roof displacement exceeding the ith limit state (LS_i) under the influence of jth intensity level (I_j).

The computation of exceedance probabilities for every intensity level yields a graph in the *PE–I* coordinate system with points that increase monotonically. This is the scattered plot form of the damage potential curve. To quantify this information better, an optimum continuous curve is usually fitted to the points. Fragility curves with a lognormal cumulative distribution were employed in this study. The ground motion intensity parameter has been selected as the peak ground acceleration (PGA) for the scope of the research project. This decision has been made primarily for two reasons. The first of these is the large number of structures in the building stock that have masonry load-carrying systems. When determining a masonry structure's fragility, it is more realistic to use a parameter that represents the structure's load-carrying capacity rather than a parameter that represents ductility or energy consumption capacity because the behavior of these types of structures is much more brittle than other types of structural systems. The second reason is that even if reinforced concrete, a structural system with a high energy consumption capacity, is employed, it is expected from surveys conducted in the region that the deformation capacities should be quite low. Given that most structures are constructed without a significant engineering service or license. For this reason, PGA is chosen as the ground motion intensity parameter for fragility functions rather than PGV or any other spectral parameter. The curves obtained are shown in Figure 47.

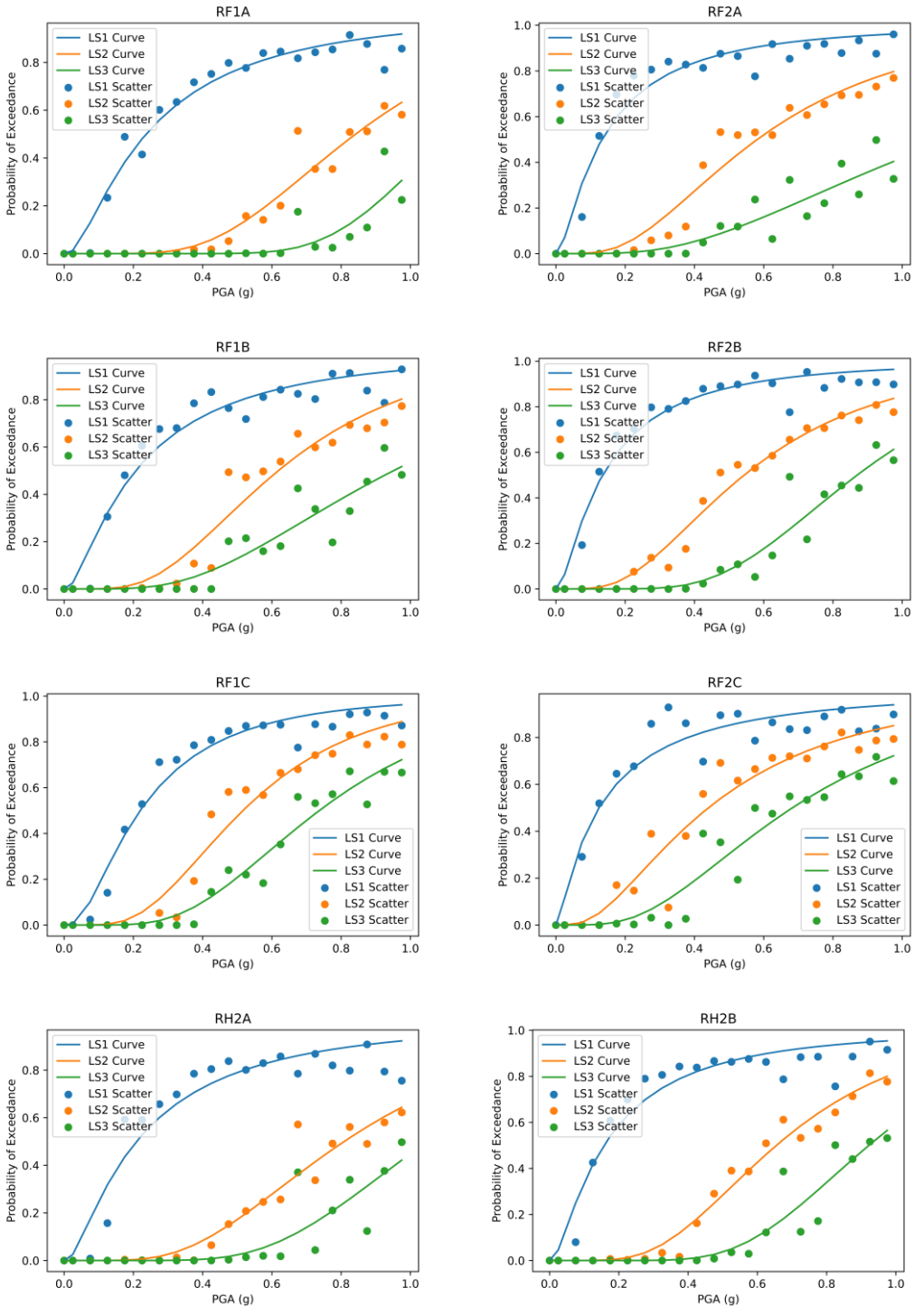

Figure 47. Generated fragility curves for each RC subclass

4.4 Comparison with the Current Parameter Set

Using the new parameter set derived in this thesis, all structural simulation analyses conducted as part of the project to assess structural vulnerability were redone, and a validation study was conducted. Computer model outputs from nonlinear analysis are idealized, as detailed in detail in Chapter 3. After that, the data was distributed among the subclasses of RC structures that were identified within the project's parameters, and the hysteretic model's mean and standard deviation values were found. Table 12 presents these figures for observation.

Table 12. Hysteretic model parameters derived in this study for each RC building subclass

	T (s)		η		μ		α_s (%)		α_c (%)	
	MN	**STD**	**MN**	**STD**	**MN**	**STD**	**MN**	**STD**	**MN**	**STD**
RF1A	0.18	0.09	0.56	0.55	9.45	5.68	5.4	16.4	-16.0	17.5
RF1B	0.20	0.10	0.36	0.39	5.73	5.36	19.9	32.2	-17.4	19.1
RF1C	0.34	0.13	0.17	0.10	5.06	4.01	19.1	31.8	-18.7	17.5
RF2A	0.50	0.13	0.16	0.07	5.63	2.94	5.5	14.0	-24.0	20.7
RF2B	0.55	0.17	0.12	0.06	4.17	3.05	16.1	27.9	-23.2	21.8
RF2C	0.59	0.18	0.08	0.05	2.94	2.78	33.4	35.8	-25.4	26.7
RH2A	0.33	0.11	0.30	0.14	7.13	3.68	5.5	12.9	-13.3	13.1
RH2B	0.38	0.14	0.23	0.12	6.06	3.77	11.1	20.2	-13.6	14.3

The main advantage of the current database is that it provides a distribution for the α_s and α_c values instead of a set value. These variables introduce a significant level of uncertainty and have a significant impact on behavior. After an in-depth review, the figures seem to be in line with previous research findings, which supports the database's consistency and dependability. This divergence from fixed values improves the database's adaptability and resilience while developing a more comprehensive understanding of the dynamic behavior impacted by α_s and α_c parameters. Corresponding updated fragility curves are represented in Figure 48.

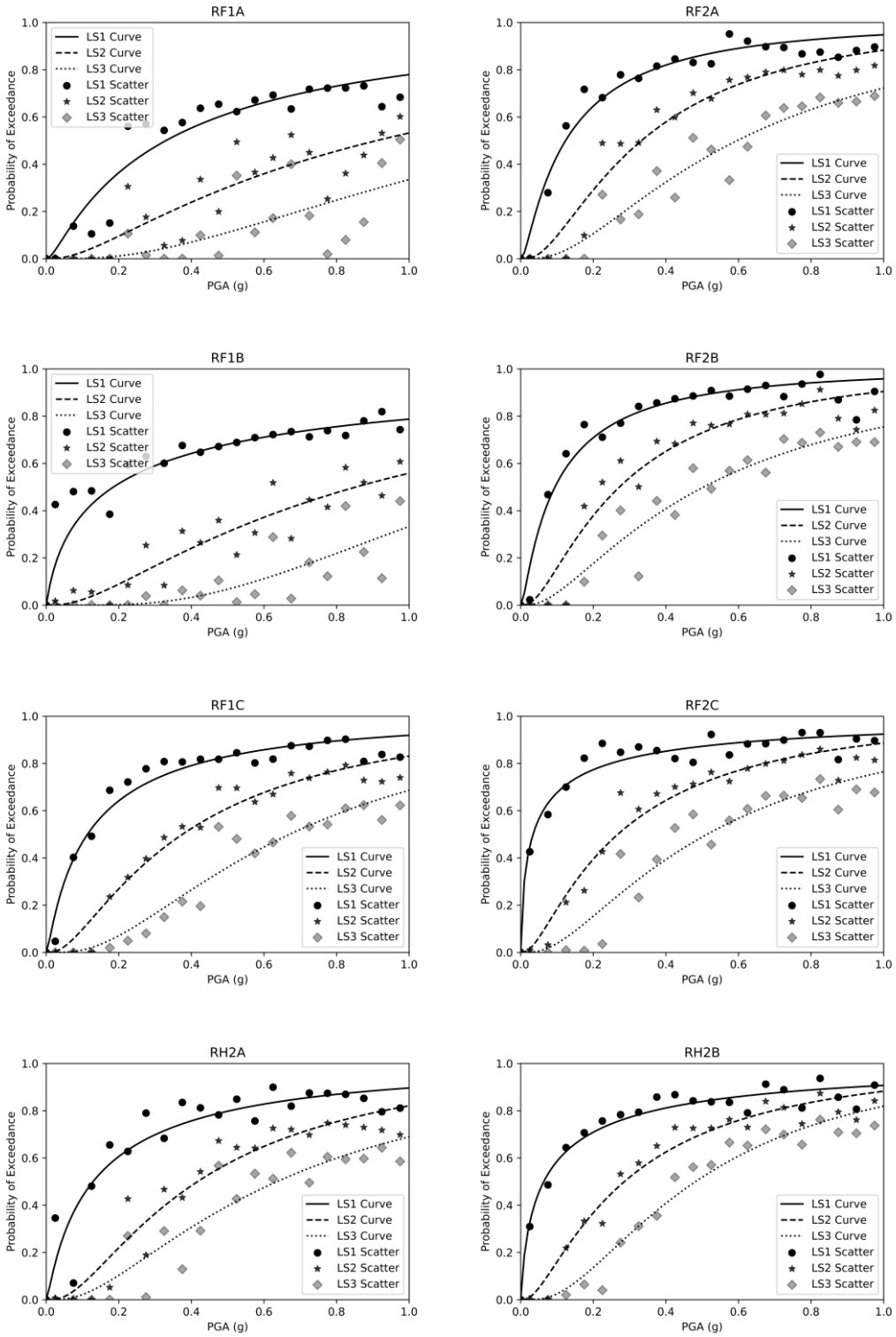

Figure 48. Fragility curves generated by using the current database for each RC subclass

Studies on fragility curves with two distinct parameter sets typically yield results that are in agreement with one another. The vulnerability of the building subclass grows dramatically in the newly obtained parameter as well as the number of stories in the structure increases and earthquake code regulation compliance declines, as expected in both the hybrid and RC frame models. The vulnerability of RC hybrid structural systems was higher than before with the use of the current parameter set. This is due to the low shear wall ratios in Turkiye's building stock and the lower base shear carrying capacity.

4.5 Regional Damage Estimations Before and After the Earthquake

One earthquake occurred on February 6, 2023, with a magnitude of Mw7.8 (USGS) and a center in Kahramanmaraş Pazarcık. Nine hours later, another earthquake with a magnitude of Mw7.5 (USGS) and a center in Kahramanmaraş Elbistan. Although some of the damaged buildings collapsed following the second earthquake, it was observed that the buildings in the Turkoglu region were particularly affected by the first earthquake. Researchers from the project team visited the Turkoglu district several times after the earthquakes to try and collect as much information as possible about the damage that they had personally seen coming from the earthquakes. As previously noted, data from the building inventory research conducted in the district before the disaster was transferred to the GIS environment. Following the earthquakes that struck Kahramanmaraş in February 2023, the work of the project team that visited the area and the damage assessment data transferred to the Disaster Coordination Information System by the Ministry of Environment, Urbanization, and Climate Change were assessed one by one by address-based scanning. The data on damaged buildings was also moved into the same GIS system (Figure 49). As a result, the buildings under investigation's pre- and post-quake damage statuses are displayed on the same map. Figure 50 shows before and after earthquake photographs of a sample building in Turkoglu.

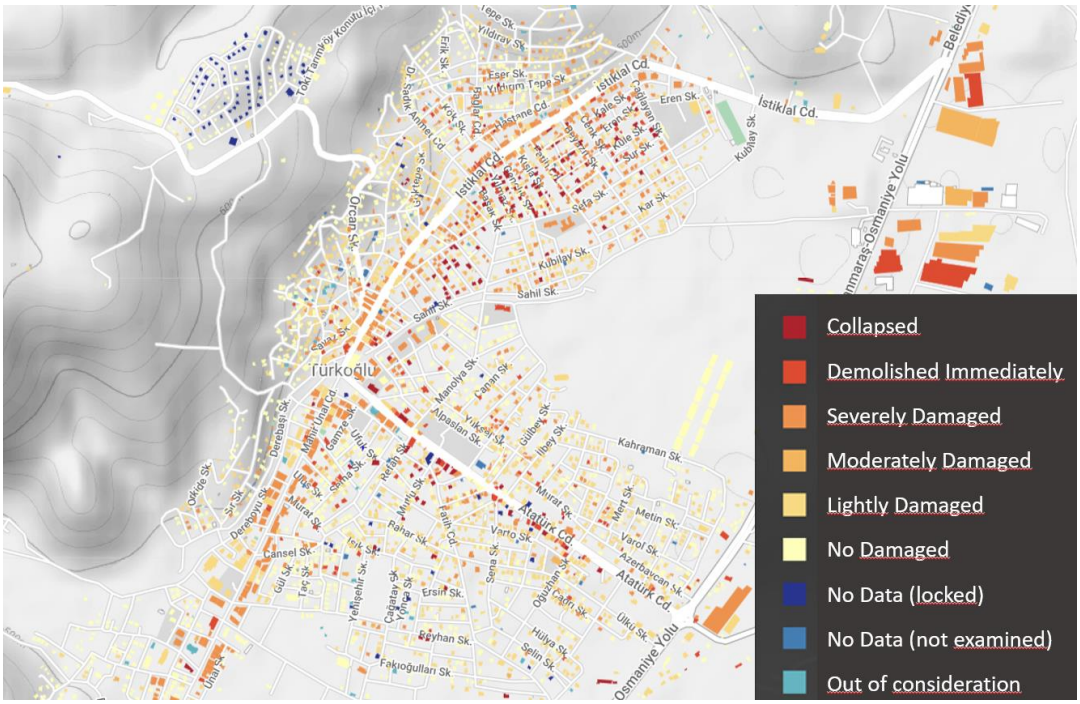

Figure 49. Damage distribution map of Turkoglu

Figure 50. An example building in Turkoglu, before and after the earthquake

The damage scenario predicted by the models was then compared with the actual damage situation observed in the area. In this case, the methodology outlined by Askan and Yucemen (2010) was applied. According to this concept, damage probability matrices (DPM) can be computed as discrete damage rates using continuous fragility functions or they can be derived directly from field measurements as empirical and discrete rates. Table 13 displays a sample damage probability matrix. Using this matrix, the intensity of the ground motion can be expressed in terms of PGA, PGV, or MMI (Modified Mercalli Intensity Scale).

Table 13. Sample damage probability matrix

Damage State (DS)	**Central Damage Ratio (%)**	**Ground Motion Intensity Parameter (I)**
No Damage	0	
Light	5	
Moderate	30	Damage Probabilities, P(DS, I)
Severe	70	
Collapsed	100	

Several damage levels have been identified by researchers or engineers, and these are vocally represented in these matrices as damage states (DS). Damage scenarios can be quantitatively represented using the damage ratio (DR), which is the ratio of any structure's repair expenses to its rebuilding costs and ranges from 0% to 100% and varies logarithmically. However, Central Damage Ratios (CDR) have been created to roughly depict each damage situation as a single figure. Instead of using the full matrix, it is important to display the state of structures at a certain earthquake intensity level with a single damage rate in cases when comparisons will be made on a regional basis, as in this study. The Mean Damage Rate (MDR) is defined as follows for this purpose.

$$MDR(I_j) = \sum_{DS} P(DS_i, I_j) \times CDR(DS_i) \quad (4.2)$$

$where$

$MDR(I_j) =$ Mean Damage Ratio under the j'th intensity level

$P(DS_i, I_j) =$ Damage probability of i'th damage state under the j'th intensity level

$CDR(DS_i) =$ Central damage ratio of the i'th damage state

Because fragility curves are given in terms of PGA in this study, damage probabilities were determined from the curves as the value that related to the associated PGA value of the corresponding earthquake in each population center. Next, the mean damage ratio (MDR) for each building class type in each district was calculated using the aforementioned algorithm. The MDR values for different building types were blended in proportion to the distribution percentages of those different building types in that region, with a single MDR value for each settlement center. Table 14 shows the estimated mean damage ratios from both fragility function sets produced by the implementation of the parameter set derived by Karimzadeh (2018) (*Estimated (Karimzadeh, 2018)*) and derived in the current study (*Estimated, (Current)*) datasets, as well as the observed mean damage ratio from the actual damage data announced by the Government following the earthquake.

Table 14. Comparison with the estimated vs. observed mean damage ratios.

MDR (%)	**DISTRICTS**					
	CUMHURİYET	**FATİH**	**GAZİLER**	**GAZİ-OSMANPAŞA**	**İSTASYON**	**KILILI**
Estimated (Karimzadeh, 2018)	43.7	44.5	45.5	43.5	40.4	38.9
Estimated (Current)	47.0	50.0	49.0	47.3	45.0	42.9
Observed (Government)	24.0	21.6	24.5	37.8	17.2	22.8

4.6 Concluding Remarks

In all neighborhoods, the actual MDR values are lower than the expected MDR values, as can be shown by comparing the observed and predicted values in Table 14. In essence, this is a required and expected circumstance. It is anticipated that the estimation methods will produce conservative conclusions since they make too many assumptions and simplify things. Furthermore, a significant number of technical staff expeditiously completed damage assessments in the field, giving administrative over academic goals priority. The distributions show that decisions about "minor damage" and "severe damage" are made more often than decisions about "moderate damage," which is what is anticipated in typical damage assessments conducted in disaster areas. Project teams noticed during this process that there were too many damaged buildings, which meant there weren't enough technical teams working in the field. As a result, less experienced teams were sent to the field, which made it sometimes impossible to determine the actual damage level.

The fact that damage assessment data released by state channels is constantly changing is another aspect contributing to this discrepancy. As a result of building users' concerns about safeguarding their property after the damage state assessed in the initial surveys following the earthquake, damage assessment classes frequently change. As an illustration, it was ruled that a structure that had been classified as moderate damage during the initial inspection could, due to objections, be reclassified as light damage and kept in operation.

The MDR values produced utilizing the Karimzadeh (2018) database were found to be lower than those produced with the database derived in this study. The fact that the average base shear force carrying capacity values of the building subclasses that surface from a thorough analysis of the new database is lower than previously is one of the primary causes of this. The MDR values determined for the regions rise as a result. However, since this method gives logarithmic results, the difference between the two databases is almost negligible. For this reason, the results of this study have been validated and its effectiveness has been proven.

CHAPTER 5

RESULTS AND CONCLUSION

The recent earthquakes have made it very clear that buildings in high-risk areas of Turkiye need to be recognized immediately, and that programs involving retrofitting or urban transformation need to get underway right now.

In the literature, there are many studies developed to determine the risk of RC buildings. They are used in various regions and for various purposes with their ease of applicability, efficiency rates, and building stock features where they can be defined and used.

A novel methodology is suggested as part of this study that can produce the most thorough and possibly the most effective risk assessment for the behavior of the Turkish building stock to date. This dataset can be used to roughly predict the capacity curve of an RC structure anywhere in Turkiye. According to the earthquake risk in the area where the building is located, the risk level of the structure can then be assessed. This methodology allows the assessment of the performance of the structure with the implementation of nonlinear response history analysis by using SDOF models with the use of idealized capacity curves. This provides researchers with great flexibility in terms of use and scope, as well as rapid risk determination.

The creation of models that accurately capture the architectural traits of the Turkish building stock is the study's most crucial stage. It should be noted that adding construction aspects unique to a given region to the structural models is the only way to develop a trustworthy seismic risk assessment. For this aim, the models included the most prevalent forms of deficiencies observed in structures, as well as the material attributes and building processes that are generally preferred in the Turkish construction industry.

The goal of this thesis study has led to the decision to focus on RC structures with one to twelve stories to account for residential buildings, which are commonly found in earthquake-prone areas of Turkiye. Also, to cover the regulations of the past four Turkish seismic codes, building models are constructed by considering the design and construction to be between the years 1975-1998, 1998-2007, 2007-2018, and 2018, respectively. Then, to ascertain the purpose of building use, occupancy class—that is, residential or non-residential use—is acknowledged as a variable. Lastly, soft story, short column, and vertical irregularities are regarded as Boolean structural irregularities. Within the parameters of this thesis study, a total of 14 parameters were sampled by assuming a statistical distribution that can describe the properties of the Turkish RC frame buildings.

After accounting for the building's structural irregularities, occupancy class, year of construction, and number of floors, 4768 RC structure subclasses were found. Using the SAP2000 analysis software, a total of 95360 structural models were created by creating 20 samples for each building subclass. Then, for every numerical model, nonlinear static pushover assessments are performed. Following the investigation, the findings of the continuous and erratic static pushover analyses were simplified and idealized by considering the guidelines outlined in FEMA356 (2000) and ASCE 41-17 (2017). In this way, a new dataset that contains capacity curves was found to represent the behavior of RC buildings containing the most common construction characteristics in Turkiye.

The structural vulnerabilities found in an earlier urban seismic resilience research in Kahramanmaraş's Turkoglu district were compared to the structural vulnerability estimations made using the new parameter set this study produced as part of the thesis work. Upon interpreting the comparison results broadly, it was noted that the new database produced results that were quite similar to those frequently found in the literature. As a result of this study, formed the basis for future structural vulnerability studies rather than assigning a direct risk score to buildings.

To briefly summarize the strengths, differences, and gaps in the literature of the results of this thesis study.

- In research on the behavior of buildings under earthquake excitation generated using nonlinear analysis methods, 2D building models are often favored since they reduce computing time; however, 3D modeling was preferred in this study.
- The models used in earlier research either neglected or only partially reflected structural deficiencies that were frequently seen in Turkiye's building stock. Nonetheless, heavy overhangs, short columns, soft stories, vertical irregularity, and plan irregularities—all of which are common in earthquake zones and significantly raise vulnerability—were taken into account within the parameters of this analysis.
- This study allowed the effects of all types of defects on the behavior of the building to be examined and interpreted separately. Normally, building defects are examined under certain groups, grouped with a parameter such as the compliance with earthquake regulations parameter, and reflected by reducing parameters like ductility or energy consumption capacity.
- Apart from the geometrical defects of the structure, the model takes into account as input parameters the building's height, material characteristics, year of construction, and usage class, all of which have a direct impact on its behavior. This would make it possible to predict Turkiye's building stock's behavior in a far more precise, realistic, and particular way.
- The sample size was limited due to the lengthy computation times of the analysis methodologies often employed in the literature that relate to this thesis study. However, 20 samples were made for each of the 4768 possible combinations that this study looked at, resulting in a total of 95360 models.

Of course, there are shortcomings in the procedures and findings presented in this thesis, as well as areas that require further research and development. These parts are listed below to draw attention to them.

- All the models developed in this thesis were predicated on a regular frame structure. Stated differently, the joints between columns and beams have conventionally been acknowledged to be perfect and continuous. Indeed, a great deal of Turkey's building stock exhibits uneven and discontinuous framing.
- The stiffness modifier values suggested by TBEC-2018 were directly applied to the models within the context of this thesis work. By permitting the usage of cracked sections, these values decrease the elastic capacity of structural parts. It also elongates the period of the structures since it reduces the stiffness of each component. This matter requires a thorough sensitivity analysis, and the impact on building capacities needs to be assessed.
- For all models, the standard slab system with RC beams was the chosen option. There are structures in Turkey with wide beams, or hollow block flooring (asmolen in Turkish), which are typically seen in structures with ground floors used for commercial purposes.
- In the context of this investigation, the range of 0.5% to 2% is considered to represent the shear wall area to floor area ratio in RC hybrid systems, or frame and wall systems. Though they are uncommon, there are certain structures with a significantly greater shear wall area ratio.
- Shear walls were placed around the building's perimeter as part of this study to facilitate the plan irregularity's integration into the system. Nevertheless, careful consideration and improvement should also be given to the behavior of various configurations, such as core shear walls.
- This thesis investigated structures of up to twelve stories. Still, far taller structures are common, particularly in urban areas. By adding more floors to the overall methodology, it is important to expand the study's scope to include the behavior of high-rise buildings.

- Within the scope of this thesis, only RC frame and RC hybrid systems were evaluated. Research should be done on a database that depicts the behavior of RC structures built using the tunnel form technique, which has been the topic of much discussion, particularly in the wake of the Kahramanmaraş earthquakes.

REFERENCES

ABYYHY-1975 (1975). Turkish Earthquake Code: *Specifications for the Buildings to be Constructed in Disaster Areas*, 1975, Ministry of Public Works and Settlement, Ankara, Turkiye. Retrieved from https://webdosya.csb.gov.tr/db/destek/icerikler/1_1_1975_deprem_yonetmel-g--20191127140243.pdf

ABYYHY-1998 (1998). Turkish Earthquake Code: *Specifications for the Buildings to be Constructed in Disaster Areas*, 1998, Ministry of Public Works and Settlement, Ankara, Turkiye. Retrieved from https://webdosya.csb.gov.tr/db/destek/icerikler/1_2_1997_deprem_yonetmel-g--20191127140319.pdf

Akkar S., H. Sucuoğlu, A. Yakut (2005). Displacement-Based Fragility Functions for Low- and Mid-Rise Ordinary Concrete Buildings, *Earthquake Spectra* 21-4; 901-927

American Society of Civil Engineers (ASCE), 2005. *Improvement of Nonlinear Static Seismic Analysis Procedures*. FEMA 440, Washington D.C.

American Society of Civil Engineers (ASCE), 2007. *Seismic Rehabilitation of Existing Buildings* (ASCE/SEI 41-06), 2007, Reston, VA.

American Society of Civil Engineers (ASCE), 2017. *Seismic Rehabilitation of Existing Buildings* (ASCE/SEI 41-17), 2017, Reston, VA.

Antoniou, S., & Pinho, R. (2004a). Advantages and limitations of adaptive and non-adaptive force-based pushover procedures. *Journal of earthquake engineering*, *8*(04), 497-522.

Antoniou, S., & Pinho, R. (2004b). Development and verification of a displacement-based adaptive pushover procedure. *Journal of earthquake engineering*, *8*(05), 643-661.

Applied Technology Council, ATC-40, 1996, *Seismic Evaluation and Retrofit of Concrete Buildings*, Volume 1-2, Redwood City, California.

Arslan Kelam A, Karimzadeh S, Yousefibavil K, Akgun H, Askan A, Erberik MA, Kockar MK, Pekcan O, Ciftci H, (2022). An evaluation of seismic hazard and potential damage in Gaziantep, Turkey using site specific models for sources, velocity structure, and building stock. *Soil Dynamics and Earthquake Engineering 154*: 107129.

Aschheim, M., & Black, E. F. (2000). Yield point spectra for seismic design and rehabilitation. *Earthquake Spectra, 16*(2), 317-335.

Askan, A., Yücemen, M.S. (2010). Probabilistic methods for the estimation of potential seismic damage: Application to reinforced concrete buildings in Turkey. *Structural Safety, 32(4): 262-271*.

Askan et al (2022). Development of a Methodology for Urban Seismic Resilience: Turkoglu, Kahramanmaras Case Study, Project final report, submitted to AFAD, July 2022 (in Turkish).

Aslani H., E. Miranda (2005). Probabilistic Earthquake Loss Estimation and Loss Disaggregation in Buildings, *The John A. Blume Earthquake Engineering Center, Report No. 157*, Department Civil and Environmental Engineering, Stanford University, Stanford, CA, USA.

Ay B.O., M.A. Erberik (2008). Vulnerability of Turkish Low-Rise and Mid-Rise Reinforced Concrete Frame Structures, *Journal of Earthquake Engineering* **12-1**; 2-11.

Aydinoğlu, M. N. (2003). An incremental response spectrum analysis procedure based on inelastic spectral displacements for multi-mode seismic performance evaluation. *Bulletin of Earthquake Engineering*, *1*(1), 3-36.

Azak, T. E., Ay, B. O., & Akkar, S. (2014). A statistical study on geometrical properties of Turkish reinforced concrete building stock. In *2nd European Conference on Earthquake Engineering and Seismology*. Istanbul Turkiye.

Badoux, M., and Peter, K. (2000) Seismic Vulnerability of Older Swiss R.C. Buildings, *Twelfth World Conference on Earthquake Engineering, January 31st – February 4th, 2000,* Auckland, New Zealand.

Bal E.İ., H. Crowley, R. Pinho (2008). Displacement-based earthquake loss assessment for an earthquake scenario in Istanbul, *Journal of Earthquake Engineering* **12-2**; 12-22.

Bal, İ. E., Crowley, H., Pinho, R., & Gulay, F. G. (2008). Detailed assessment of structural characteristics of Turkish RC building stock for loss assessment models. *Soil Dynamics and Earthquake Engineering*, *28*(10-11), 914-932.

Biggs, John M. (1964) Introduction to structural dynamics. 276-314.

Boore, D. M., Stewart, J. P., Seyhan, E., & Atkinson, G. M. (2014). NGA-West2 equations for predicting PGA, PGV, and 5% damped PSA for shallow crustal earthquakes. *Earthquake Spectra*, *30*(3), 1057-1085.

Chopra, A. K., & Goel, R. K. (2002). A modal pushover analysis procedure for estimating seismic demands for buildings. *Earthquake engineering & structural dynamics*, *31*(3), 561-582.

Chopra, A. K., Goel, R. K., & Chintanapakdee, C. (2004). Evaluation of a modified MPA procedure assuming higher modes as elastic to estimate seismic demands. *Earthquake Spectra*, *20*(3), 757-778.

Crowley H., J.J. Bommer (2006). Modeling Seismic Hazard in Earthquake Loss Models with Spatially Distributed Exposure, *Bulletin of the Seismological Society of America* **4-3**; 249-273.

Computers and Structures Inc. (CSI), 1998, *SAP2000 Three Dimensional Static and Dynamic Finite Element Analysis and Design of Structures V7.40N*, Berkeley, California.

Demircioğlu M.B., M. Erdik, U. Hancilar, E. Harmandar, Y. Kamer, K. Sesetyan, C. Tuzun, C. Yenidogan, A.C. Zulfikar (2010). Earthquake Loss Estimation Routine ELER v3.0 Technical Manual, *Network of Research Infrastructures for European Seismology*.

Erberik M.A. (2008a). Fragility-Based Assessment of Typical MidRrise and Low-Rise RC Buildings in Turkey, *Engineering Structures* **37-3**; 1360-1374.

Erberik M.A. (2008b). Generation of Fragility Curves for Turkish Masonry Buildings Considering In-Plane Failure Modes, *Earthquake Eng. and Structural Dynamics* **37-3**; 387-405.

Erberik M.A., Elnashai AS (2004). Fragility analysis of flat-slab structures. *Engineering Structures, 26*: 937-948.

Erberik, M. A., & Elnashai, A. S. (2006). Loss estimation analysis of flat-slab structures. *Natural Hazards Review*, *7*(1), 26-37.

Fajfar, P., & Fischinger, M. (1988, August). N2-A method for non-linear seismic analysis of regular buildings. In *Proceedings of the Ninth World Conference in Earthquake Engineering* (Vol. 5, pp. 111-116).

FEMA (Federal Emergency Management Agency) (2000). FEMA356, Prestandard, and commentary for the seismic rehabilitation of buildings. *Federal Emergency Management Agency: Washington, DC, USA*.

FEMA (Federal Emergency Management Agency) (2003). HAZUS, Earthquake Loss Estimation Methodology: Technical Manual MR4. *Federal Emergency Management Agency, Washington, DC, USA*.

Fintel, M. (1995). Performance of Buildings with Shear Walls in Earthquakes of the Last Thirty Years, *PCI Journal, May-June*, pp. 62-80.

Freeman, J. R. (1932). Earthquake damage and earthquake insurance: studies of a rational basis for earthquake insurance also studies of engineering data for earthquake-resisting construction, *1st Ed., McGraw-Hill*, New York.

Freeman, Sigmund A. "Review of the development of the capacity spectrum method." *ISET Journal of Earthquake Technology* 41.1 (2004): 1-13.

Gulkan, P., & Sozen, M. A. (1974, December). Inelastic responses of reinforced concrete structure to earthquake motions. In *Journal proceedings* (Vol. 71, No. 12, pp. 604-610).

Gupta, B., & Kunnath, S. K. (2000). Adaptive spectra-based pushover procedure for seismic evaluation of structures. *Earthquake Spectra*, *16*(2), 367-391.

Ibarra LF, Krawinkler H, (2005). Global collapse of frame structures under seismic excitations. Rep. No. TB 152, The John A. Blume Earthquake Engineering Center, Stanford University, Stanford, CA.

Ibarra LF, Medina RA, Krawinkler H, (2005). Hysteretic models that incorporate strength and stiffness deterioration. *Earthquake Engineering and Structural Dynamics 34*: 1489–1511.

Işık, E. (2021). A comparative study on the structural performance of an RC building based on updated seismic design codes: Case of Turkiye. *Challenge*, *7*, 123-134.

Kale, Ö., Akkar, S., Ansari, A., & Hamzehloo, H. (2015). A ground- motion predictive model for Iran and Turkey for horizontal PGA, PGV, and 5% damped response spectrum: Investigation of possible regional effects. *Bulletin of the Seismological Society of America*, *105*(2A), 963-980.

Karimzadeh S, Askan A, Erberik MA, Yakut A, (2018). Seismic damage assessment based on regional synthetic ground motion dataset: a case study for Erzincan, Turkey. *Natural Hazards 92(3):* 1371-1397.

Kirçil, M. S., & Polat, Z. (2006). Fragility analysis of mid-rise R/C frame buildings. *Engineering Structures*, *28*(9), 1335-1345.

Korkmaz, A., & Johnson, P. A. (2007). Probabilistic seismic structural assessment. In *Computing in Civil Engineering (2007)* (pp. 297-305).

Küçükçoban S. (2004). Development of a Software for Seismic Damage Estimation: Case Studies, *MS Thesis, Civil Engineering Department, Middle East Technical University, Ankara Turkey*.

Leslie, R. (2013). The pushover analysis, explained in its simplicity. In *National Conference (Recent Advances in Civil Engineering) RACE* (Vol. 13).

Lignos, DG, Krawinkler H, (2011). Deterioration modeling of steel components in support of collapse prediction of steel moment frames under earthquake loading. *Journal of Structural Engineering, ASCE, 137 (11)*: 1291-1302.

Lignos, DG, Krawinkler H, (2012). Development and Utilization of Structural Component Databases for Performance-Based Earthquake Engineering. *Journal of Structural Engineering, ASCE, 139 (8*): 1382-1394.

Mander, J. B., Dutta, A., & Kim, J. H. (1998). Fatigue analysis of unconfined concrete columns. In *Fatigue analysis of unconfined concrete columns* (pp. 146-146).

McKay MD, Conover WJ, Beckman RJ (1979). A Comparison of Three Methods for Selecting Values of Input Variables in the Analysis of Output from a Computer Code. *Technometrics, 21*: 239-245.

McKenna, F. (2011). OpenSees: a framework for earthquake engineering simulation. Computing in Science and Engineering 13, 58–66.

Meral, E. (2019). Evaluation of Structural Properties of Existing Turkish RC Building Stock. *Iranian Journal of Science and Technology, Transactions of Civil Engineering*, *43*, 445-462.

Motazedian, D., & Atkinson, G. M. (2005). Stochastic finite-fault modeling based on a dynamic corner frequency. *Bulletin of the Seismological Society of America*, *95*(3), 995-1010.

Ozmen, H. B., Inel, M., Meral, E., & Bucakli, M. (2010). Vulnerability of low and mid-rise reinforced concrete buildings in Turkey. In *Proceedings of the 14th European conference on earthquake engineering, Ohrid, Macedonia*.

Ozmen, H. B., Inel, M., Senel, S. M., & Kayhan, A. H. (2015). Load carrying system characteristics of existing Turkish RC building stock. *International Journal of Civil Engineering*, *13*(1), 76-91.

Paret, T. F., Sasaki, K. K., Eilbeck, D. H., & Freeman, S. A. (1996, June). Approximate inelastic procedures to identify failure mechanisms from higher mode effects. In *Proceedings of the Eleventh World Conference on Earthquake Engineering* (Vol. 2).

Qi, X., & Moehle, J. P. (1991). *Displacement design approach for reinforced concrete structures subjected to earthquakes*. Earthquake Engineering Research Center, College of Engineering/University of California.

Saiidi, M., & Sozen, M. A. (1981). Simple nonlinear seismic analysis of R/C structures. *Journal of the Structural Division*, *107*(5), 937-953.

Sasaki, K. K., Freeman, S. A., & Paret, T. F. (1998, May). Multimode pushover procedure (MMP)—A method to identify the effects of higher modes in a pushover analysis. In *Proceedings of the 6th US national conference on earthquake engineering, Seattle, Washington*.

Seifi, M., Noorzaei, J., Jaafar, M. S., & Panah, E. (2008). Nonlinear static pushover analysis in earthquake engineering: State of development. In *Proceeding of International Conference on Construction Building Technology, Kuala Lumpur*.

Shibata, A., & Sozen, M. A. (1976). Substitute-structure method for seismic design in R/C. *Journal of the Structural Division*, *102*(1), 1-18.

Smyth A.W., G. Altay, G. Deodatis, M. Erdik, G. Franco, P. Gulkan, H. Kunreuther, H. Luş, E. Mete, N. Seeber, Ö. Yüzügüllü (2004). Probabilistic Benefit-Cost Analysis for Earthquake Damage Mitigation: Evaluating Measures for Apartment Houses in Turkey, *Earthquake Spectra* **20-1**; 171-203.

Takeda, T., Sozen, M. A., & Nielsen, N. N. (1970). Reinforced concrete response to simulated earthquakes. *Journal of the Structural Division*, *96*(12), 2557-2573.

TBEC (2018). Turkish Building Earthquake Code. *Disaster and Emergency Management Presidency of Turkiye (AFAD), Ankara, Turkiye*.

TEC (2007). Turkish Earthquake Code 2007: *Specifications for the Buildings to be Constructed in Disaster Areas*, 2007, Ministry of Public Works and Settlement, Ankara, Turkiye. Retrieved from https://www.resmigazete.gov.tr/eskiler/2007/03/20070306-3-1.pdf

Titiksh, A. (2017). Effects of irregularities on the seismic response of a medium rise structure. *Asian Journal of Civil Engineering (BHRC), 18*(8), 1307-1314.

TS498. Design loads for building, Standard TS498. *Turkish Standards Institution, Ankara, Turkiye*.

TS500-2000. Requirements for Design and Construction of Reinforced Concrete Structures, Standard TS500. *Turkish Standards Institution, Ankara, Turkiye*.

Turkish Standard Institute (1997). Turkish Standard, TS498: The Calculation Values of Loads Used in Designing Structural Elements. *Turkish Standards Institution, Ankara, Turkiye.*

Ugurhan B., A. Askan, M.A. Erberik (2011). A Methodology Loss Estimation in Urban Regions Based on Ground Motion Simulations, *Bulletin of the Seismological Society of America* **101-2**; 710-725.

Wald D.J., P.S. Earle, T.I. Allen, K. Jaiswal, K. Porter, and M. Hearne (2008). Development of the U.S. Geological Survey's PAGER system (Prompt Assessment of Global Earthquakes for Response). Proc. 14th World Conf. Earthq. Eng., Beijing, China, 8pp.

Wyss M., G. Trendafiloski, Ph. Rosset (2009). Rapid Earthquake Casualty Estimates for Developing Countries, *Second International Workshop on Disaster Casualties*, Cambridge, June 2009.